

**TNO** report

TNO 2017 R11589

Vector sensors and acoustic calibration procedures

Oude Waalsdorperweg 63 2597 AK Den Haag P.O. Box 96864 2509 JG The Hague The Netherlands

www.tno.nl

T +31 88 866 10 00 F +31 70 328 09 61

Date December 2019

Author(s) Ir. H.W. Jansen

E. Brouns MSc Dr. M.K. Prior

Number of pages 54 Number of appendices 0 Sponsor SMO

Project name Particle motion

Project numbers 060.28733 / 060.34705

## All rights reserved.

No part of this publication may be reproduced and/or published by print, photoprint, microfilm or any other means without the previous written consent of TNO.

In case this report was drafted on instructions, the rights and obligations of contracting parties are subject to either the General Terms and Conditions for commissions to TNO, or the relevant agreement concluded between the contracting parties. Submitting the report for inspection to parties who have a direct interest is permitted.

© 2019 TNO

# Summary

The measurement of underwater sound for the purpose of environmental impact studies usually only involves the measurement of the sound pressure by hydrophones. Sea mammals are sensitive to sound pressure in water like land mammals are for sound pressure in air. However, some species of fish and invertebrates are also sensitive and responsive to sound particle motion (PM) in terms of the sound particle acceleration. Therefore there is a need for measuring, standardization, calibration and assessment of particle motion.

Particle motion can be measured directly by a vector sensor that contains sound pressure and acceleration sensors. An inventory of commercially available vector sensors was made and one vector sensor with suitable specifications for bioacoustic research has been purchased by the Acoustics and Sonar department of TNO.

A calibration procedure for vector sensors has been developed. It comprises a dry part, on an electro-dynamic shaker, and a wet part in a semi-anechoic basin. This procedure has been applied on two different types of vector sensors, which differ in terms of geometrical dimensions, weight and suspension. The importance of buoyancy and suspension aspects and phase-match between pressure and particle acceleration in the calibration procedure is shown.

With the calibrated vector sensor two field measurements have been conducted. The field test reflect two use cases for industrial activities at sea resulting in underwater sound: seismic surveys and marine pile driving in shallow water. In these experiments the method of deployment of a vector sensor was studied. Additionally, the conversion (assuming plane wave conditions) of sound pressure measured with a single hydrophone to particle motion is studied. This conversion is subject to large errors when a point source with frequencies below 1 kHz is used, but shows good potential for a line source like a marine pile driver. Also some examples of directivity aspects of vector sensors are shown.

Finally the vector sensor is connected to a stand-alone 4-channel underwater sound recorder, which allows monitoring of sound particle motion and sound pressure close to the sediment over longer period of time. The viability of this system was tested in a field test and in the semi-anechoic basin.

The vector sensor of TNO is operational now and can be used in bio-acoustic projects, in the field of the sensitivity of wildlife to acoustic particle motion generated by anthropogenic sound sources in the sea.

# Contents

	Summary	2
1	Introduction	4
2	Vector sensors	6
2.1	Introduction	6
2.2	Definition of particle motion quantities	6
2.3	Vector sensor	7
2.4	Intended use of the vector sensor	8
2.5	Requirements	8
2.6	Overview vector sensors	9
2.7	VHS-100 sensor of Ocean Applied Acoustics	11
3	Calibration procedures	
3.1	Shaker Method	
3.2	Pressure gradient method	
3.3	Free-Field Comparison method	
3.4	Self-noise	18
4	Calibration results vector sensor	
4.1	VHS-100	
4.2	M20 sensor	
4.3	Discussion	33
5	Field tests	
5.1	Introduction	
5.2	Shallow Inland waterway	
5.3	North Sea	
5.4	The effect of tidal flow on the background noise level	
5.5	Discussion	39
6	Directionality of sound	
6.1	Basin test	
6.2	Field tests	42
7	Stand-alone vector sensor recording system	
7.1	Technical description	
7.2	Calibrations	
7.3	Field test	48
8	Conclusions	51
9	References	53
10	Signature	54

## 1 Introduction

The measurement of underwater sound for the purpose of environmental impact studies usually only involves the measurement of the sound pressure by hydrophones. Sea mammals are sensitive to sound pressure in water like land mammals are for sound pressure in air. However, some species of fish and invertebrates are also sensitive and responsive to particle motion (*PM*) in terms of the sound particle acceleration. Therefore there is a need for measuring, standardization, calibration and assessment of particle motion.

This work has been performed within the Research Cooperation Funds as provided by the Ministry of Economic Affairs. This report covers two successive SMO projects on particle motion in the period 2017-2019. The objectives of the projects are to:

- Preparing and supporting the purchase of a vector sensor by the Acoustics&Sonar Department of TNO.
- Design and test a calibration procedure for vector sensors.
- Determine the added value of vector sensors for bio-acoustics, when and why
  are hydrophone measurements not sufficient.
- Design, assemble and test a stand-alone monitoring system for vector sensors.

At the start of the first project the Acoustics and Sonar department of TNO did not own any vector sensors. Therefore the project started with making an inventory of commercially available vector sensors, see Chapter 2. After this desk study a suitable vector sensor was selected and purchased <sup>1</sup>.

Since standardized calibration procedures on sound particle acceleration do not exist, calibration procedures are proposed in Chapter 3. The procedure comprises a dry part, in air, and a wet part in a water basin. Some of these calibrations are performed in the acoustic basin of TNO on two different vector sensors and the results are compared, see Chapter 4.

The particle motion research continued with a follow-up of the previous project. The calibration procedures are validated with a popular vector sensor in the bio-acoustic field. Since this sensor deviates from the TNO sensor regarding weight, dimensions and suspension, it allows validation of the compliance of dry and wet calibrations. This is reported in Section 4.2.

Until this phase of the project only laboratory measurements have been performed. As a next step field tests were performed with the vector sensor in a shallow inland water-way and at the North Sea, see Chapter 5. This work has also been presented at the International Aquatic Noise conference and published in the Proceedings of Acoustic Meetings of the Acoustical Society of America as a part of the dissemination.

The fact that vector sensor are sensitive to the directionality of sound waves is illustrated in Chapter 6 by laboratory and field experiments.

A second vector sensor was purchased by the A&S department. However, since this sensor and all results obtained with it fall under strict US ITAR regulations, details on this sensor are reported in a separate memo [14] which cannot be distributed outside TNO.

Finally the vector sensor is connected to a stand-alone underwater sound recorder, which allows monitoring of sound particle motion and sound pressure close to the sediment over longer periods of time, see Chapter 7. The validity of this system was tested in a field test and in the acoustic basin. This report ends with conclusions in Chapter 8.

# 2 Vector sensors

#### 2.1 Introduction

This chapter starts with information about particle motion in relation to sound pressure and the detection of particle motion by vector sensors in Sections 2.2 and 2.3. The intended use of TNO of the vector sensor is defined in Section 2.4, resulting in requirements in Section 2.5. Section 2.6 gives an overview of commercially available vector sensors, partly found in the bio-acoustic literature.

## 2.2 Definition of particle motion quantities

Particle motion can be expressed in terms of displacement, velocity or acceleration and is the contribution to instantaneous motion of a material element due to the action of sound waves [12]

For a free field plane wave, it can be shown that the particle acceleration a and the sound pressure p are related by the linearized version of the Navier-Stokes equation for a Newtonian fluid [2]:

$$-\nabla p = \rho_0 a \tag{2.1}$$

with  $\rho_0$  the density of the medium in kg/m3.

Further, for a propagating plane wave there is a relationship between the sound pressure p and particle velocity v:

$$v = \frac{p}{\rho_0 c_0} \tag{2.2}$$

with  $c_0$  the compressional speed of sound in the medium in m/s and  $\rho_0$  the density in kg/m<sup>3</sup>.

The product of  $\rho_0 c_0$  is called the characteristic specific acoustic impedance  $Z_0$  in Pa·s·m<sup>-1</sup>. It is a property of the medium and is, for example, different for salt water than for fresh water. The characteristic specific acoustic impedance can also be determined by using a CTD probe measurement, which measures the conductivity, temperature and pressure of the surrounding medium. The speed of sound, the density and the corresponding impedance can be determined from these properties.

Eq. (2.2) allows a simple conversion of measured sound pressure into particle velocity. However, free-field propagation conditions are not always met in shallow waters or a laboratory tank, and the conversion may be subject to a significant error. To overcome this error the sound particle motion can be measured directly with a vector sensor.

The sound particle acceleration level La is defined in ISO18405 [12]:

$$L_a = 10 \log_{10} \left( \frac{1}{T} \int_0^T \left| \frac{a(t)}{a_0} \right|^2 dt \right) dB$$
 (2.3)

*T* is the averaging time in [s] and the reference value of the sound particle acceleration,  $a_0^2$ , is 1 ( $\mu$ m/s²)² and a(t)² is calculated from:

$$a(t)^{2} = a(t)_{x}^{2} + a(t)_{y}^{2} + a(t)_{z}^{2}$$
(2.4)

The values of a(t) are measured using the particle motion sensor. This equation shows that particle motion requires vector rather than scalar measurements.

Besides the sound particle acceleration level there is also a need for a way to quantify the sound pressure to particle motion conversion. In this report the *scaled impedance* metric  $Z_{sc}(f)$  is proposed as a way to quantify the conversion following the plane wave relationship of eq. (2.2). It is defined is the measured impedance normalized to the measured characteristic specific impedance  $\rho_0 c_0$ ,

$$Z_{sc}(f) = \frac{p(f)}{u(f)\rho_0 c_0} \tag{2.5}$$

Where u(f) is defined as the resulting vector, composed of the vectors in each orthogonal directions  $u_x$ ,  $u_y$  and  $u_z$ :

$$u(f) = \sqrt{u_x^2 + u_y^2 + u_z^2} \tag{2.6}$$

The level of scaled impedance can also be defined on a decibel scale:

$$L_{Z_{SC}} = 10\log_{10}|Z_{SC}|^2 \, \text{dB} \tag{2.7}$$

In this case the scaled-impedance levels can be calculated from the sound pressure level  $L_p$  and particle velocity level  $L_u$ :

$$L_{Z_{sc}} = L_p - L_u - 20\log_{10}(\rho_0 c_0) \, dB \tag{2.8}$$

It can be used as a metric for the conversion of sound pressure to particle velocity. If  $L_{Z_{sc}}$  approaches 0 dB the actual impedance is about equal to the characteristic specific impedance. This indicates that free-field conditions are being experienced. When  $L_{Z_{sc}}$  becomes negative the calculated particle velocity u, following eq. (2.5), is underestimated. When  $L_{Z_{sc}}$  is positive, u is overestimated.  $L_{Z_{sc}}$  indicates the accuracy of the free-field conversion of sound pressure to particle motion. The acceptability of this accuracy will depend on the actual application.

#### 2.3 Vector sensor

Detection of particle motion requires different types of sensors than those applied for the measurement of sound pressure by a conventional hydrophone [5, 6]. Particle motion requires vector rather than scalar measurements [1]. Therefore the

term *vector sensor* is often used for such sensors. Whereas hydrophones are widely available and easy to deploy, there are far fewer sensors for particle motion commercially available. Also specials skills in their use are required, such as deployment method, mounting and calibration. The sound particle acceleration can be measured directly by a dedicated vector sensor, which can measure the particle acceleration in multiple directions by tri-axial accelerometers [5]. Vector sensors also contains a hydrophone element with the same phase center as the accelerometers.

#### 2.4 Intended use of the vector sensor

The intended use of the vector sensor within the Acoustics and Sonar department is to participate in research in the field of the sensitivity of fish and invertebrates to acoustic particle motion with goals to:

- determine the amplitude level of the sound particle motion in relevant frequency range in laboratory and field experiments;
- determine ambient sound particle motion levels in the sea;
- determine sound particle motion near anthropogenic sources (e.g. ships, airgun, pile driver).

## 2.5 Requirements

For this intended use the following requirements are set for the vector sensor:

#### Frequency range of frequency band

Concerning particle motion the frequency range between 50 Hz and 2 kHz is the most relevant for a majority of fish and invertebrate hearing studies [2]. However, some fish are sensitive to particle motion at lower frequencies down to 20 Hz [3]. Therefore the required frequency range is set to: **20 Hz to 2 kHz.** 

## Self-noise level

For frequencies beyond 500 Hz, the ambient sound acceleration levels in the ocean can be derived from the Wenz curves. The Wenz curves describe the ambient underwater sound pressure levels in third-octave bands for various sea-states. The ambient sound is governed by wind and waves at the sea surface. The sound velocity levels can be derived from these sound pressure levels assuming plane wave propagation under free-field conditions, following eq. (2.2). Next, acceleration levels follow by subtracting of  $20\log_{10}(2\pi f)$  in the frequency domain; see Figure 2.1.

When measured self-noise levels of the pressure and acceleration channels of the vector sensors, in connection to the data-acquisition system, are overlaid in these plots, it becomes clear at which sea state the sensor is still able to measure the ambient sound particle acceleration. For ambient sound particle measurements during sea state 1 condition the self-noise levels need to be close to the background noise levels of sea state 0. For measurements near a pile driver or a seismic survey higher self-noise levels are acceptable, depending on the measurement distance from the source.

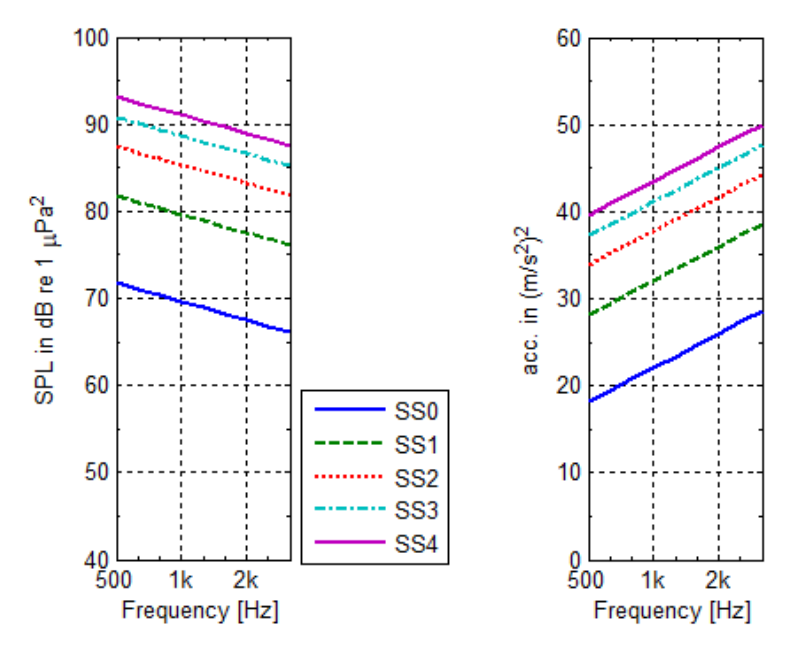


Figure 2.1 Acceleration levels (right) derived from the free-field sound pressure levels (left) as defined in the Wenz curves, in third-octave bands.

#### Orientation

Since vector sensors measure the particle motion in three orthogonal directions, the orientation of the vector sensor's coordinate system and its polarity need to be known and fixed. Some vector sensors have a digital compass with orientation sensors onboard for this purpose. If these sensors are not onboard, external heading, pitch and roll sensors can be co-located with the vector sensor, see also Chapter 7.

#### Mounting

To measure the amplitude of the acceleration of the moving water particles, the suspension system of a vector sensor is critical. It serves as a basis to fix the average position and orientation of the sensor body and allows free movement of the sensor body in response to the acoustic field. At the same time the sensor is isolated from structure-borne sound traveling through the mounting structure, potentially contaminating the measurement signals. Since the mass of the submerged sensor and the suspension stiffness becomes a resonating system, its resonant frequency should be designed outside the measurement frequency range of interest. In view of the specified lower frequency limit of 20 Hz, the design frequency of the resonating system should be minimal 14 Hz. Overview vector sensors.

#### 2.6 Overview vector sensors

Most of the commercially available vector sensors are inertial motion sensors, also called P-A vector sensors [1]. This type of vector sensor works by physically measuring the movement of the water in the presence of a sound field. This is achieved using accelerometers mounted within a rigid spherical shell (sensor casing). The whole structure usually is slightly negatively buoyant and free to follow the movement of the water. Table 2.1 gives an overview of commercially available vector sensors.

Table 2.1 Overview of commercially available vector sensors with properties and specifications.

Supplier	Туре	Peak Acceleration	Peak Band pressure/acc, width	Band width	Sensitivity	_ ,,	Power I supply	Dimensions	Dimensions Orientation Weight sensor [kg in a	Ē	Price KEUR	Delivery tim ITAR months	ITAR
Geospectrum	MZO 6	gain depending		10 Hz - 3 kHz	gain depending			Ø12.7cm;			ę	2.5	e
Vilcoxon	VS-301	5 m/s 2 (134 dB re 1 um/s 2)	175 dB re 1 uPa	3 Hz - 2 kHz	pressure: -1f	-162 dB re 1uPa 6 1V/m/s2	6.5-9 VDC (		sek	0.04	₽	2	yes
	VS-209	10 m/s2 (140 dB re 1 um/s2)	166 dB re 1 uPa	3 Hz - 7 kHz	pressure: -16 acc. 0.1	-164 dBre1 uPa 0.15 V/m/s2	6.5-12 VDC 40 mA	Ø4cm; H7cm	serk	0.1	P P	2	sex
	101-SA	5m/s2 (134 dB re 1 um/s2)	166 dBre 1 uPa	3 Hz - 2 kHz	pressure: -16 aoc. 0.6	-162 dB re TuPa 0.6 Wm/s2	3-9VDC 30 mA	Ø7.6cm; H19cm	sek	0.7			yes
	VS-403	150 m/s2 (134 dB re 1 um/s2)	190 dB re 1 uPa	1Hz - 20kHz	pressure: -2 acc. 3r	-202 dB re 1 uPa 6.5-9 VDC 3 m Vimis 2 15 m A		Ø1.5 cm; H3.6 cm	seń	0.011			yes
Ocean applied acoustics	001-SHA	VHS-100 1.5 kPa (184 dB re 1 μPa). 8 m/s² (138 dB re 1μ m/s2)	ı	20 Hz- 4 kHz	pressure: -18 acc. 0.3	-180 dB re 1uPa 1	18-28 V DC (	Ø3cm	00	0.4	12	1.5	2
	VHS-58	4.8kPa (194 dB re 1μPa). 25 mls² (148 dB re 1μ mls2)		100 Hz - 7 kHz	pressure: -16 acc. 80	-190 dB re 1uPa 2 80 mV/m/s2	24 V	Ø5.8 cm	٤	0.1	δ	ო	2
Micro-Fine Acoustic Vector Sensor	AVS120	unknown		100 Hz - 3 kHz	pressure: -1{ acc. 12	-194 dB re 1 uPa 12 mV/m/s2		Ø6.5 cm	00		6	2-3	e e

One alternative approach to measuring vector sound field quantities is based on a principle used in hot wire anemometry. These sensors measure the change in electrical resistance of a heated wire. The particle velocity is obtained from the relationship between this electric resistance and the convective effects of flow around the wires. MICROFLOWN in The Netherlands developed a sensor to measure the particle motion in air, and is currently developing a sensor for the measurement of particle motion in water.

The US sensors of Wilcoxon are considered as military goods by the US government and require special US permits (ITAR) to export the vector sensor for measurements campaigns, but also to share technical specifications and measurement data and results.

The M20 sensor of Geospectrum is found frequently in the bio-acoustic literature. The sensor is relatively large and heavy (mass 4 kg in air, 17 cm length, 13 cm diameter) and has a specific gravity of 1.9. How this affects the ability to measure particle motion is discussed in Chapter 4.2. The Bio-Acoustic lab of the University of Leiden (IBL) owns an M20 sensor. TNO has calibrated this sensor and compared the specifications and performance with the VHS-100.

In order to learn more about the types of vector sensors, TNO consulted some international experts by e-mail, skype and face-to-face meetings:

- Bruce Martin, Applied Sciences Manager at JASCO Applied Sciences, experienced M20 user. He shared his experiences and pitfalls with the M20 and has sent a technical report with details on this sensor [10].
- Peter Rogers, Professor Emeritus, GeorgiaTech; experience with Wilcoxon VS-101 sensor, designed vector sensor for the US Navy.
- Peter Dahl, Senior Principal Engineer, Acoustics Department of the Applied Physics Laboratory, Seattle USA, experience with VHS-100 sensor. He shared his experiences, the sensitivities obtained from an in-house calibration and their solution of a mooring frame for long-term monitoring.

TNO decided to purchase the VHS-100 sensor of Ocean Applied Acoustics. This sensor is also used by Acoustics Department of the Applied Physics Laboratory, Seattle. The next section gives more information about this sensor.

## 2.7 VHS-100 sensor of Ocean Applied Acoustics

The spherical vector sensor VHS-100 is made of three pairs of accelerometers set in three orthogonal directions. These sensors are fixed onto a base block and sealed into an epoxy ball; see Figure 2.2 and Figure 2.3. To keep the vector sensor in suitable orientation with elastic bands, three pairs of fixing rings are attached on the outside of the epoxy ball.

The external pre-amps of the accelerometers are powered by a 24V battery. The sensitivity of the accelerometers is 250 mV/m/s² (-12 dB re 1V/m/s²). The separate acoustic pressure channel (-178 dB re 1 V/ $\mu$ Pa) measures the underwater sound pressure.

According to specifications the preamplifier of the VHS-100 saturates at a peak voltage level of 2 V. This corresponds to a peak acceleration of 8 m/s<sup>2</sup> (138 dB re  $1\mu$  m/s<sup>2</sup>) and a peak pressure of 1.5 kPa (184 dB re  $1\mu$ Pa).

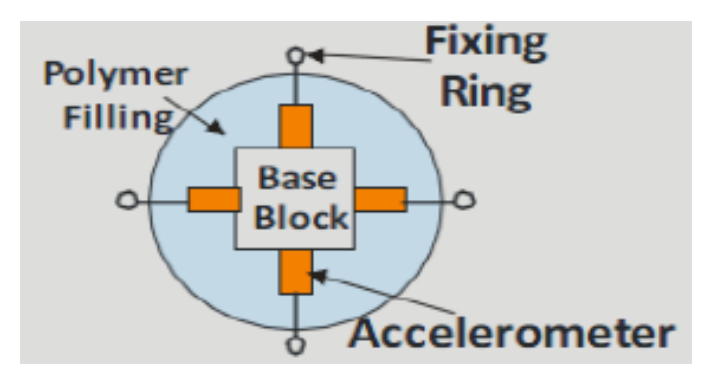


Figure 2.2 Schematic overview of the VHS-100 vector sensor. In each direction a set of two accelerometers are installed.



Figure 2.3 Overview of the vector sensor (orange sphere), signal conditioner with pre-amplifiers (steel cylinder) and suspension cage (right).

The weight of the sensor equals 0.465 kg in air and 82 g in water. The radius of the sphere is 0.045 m. This results in a density of 1218 kg/m<sup>3</sup>, and a specific gravity  $\gamma = \rho_{pm}/\rho_{H_2O} = 1.2$ .

The sensor comes with a suspension system, consisting of elastic bands, constraining the vector sensor in an aluminum cage. The natural frequency of the mass-spring system (the ball in the elastic suspension) is 10 Hz in air. Also in water the natural frequency is expected to be 10 Hz, when taking into account the added mass of the moving water volume. This makes the sensor usable from about 20 Hz, which is according to specification. If measurement of particle motion at lower frequencies is required, a softer suspension system is needed.

The calibration of the sensor was performed at the facilities of Hangzhou Applied Acoustics Research Institute (HAARI) in China by the comparison method, see also Chapter 3. The size of the used basin is 50 m by 15 m and a depth of 10 m.

#### 2.7.1 Sensitivity of the VHS-100 sensor

The manufacturer of the VHS-100 sensor expresses the sensitivity of the accelerometers ( $m_a$  in V/m/s²) and the sensitivity to the sound pressure in an equivalent plane wave ( $m_{p,eq}$  in  $\mu$ V/Pa). However, for an accelerometer it is preferred to express its sensitivity in the unit corresponding to the physical quantity, which is m/s². Therefore the sensitivities of the specifications are converted by the following expression:

$$m_a = \frac{\rho c m_p}{2\pi f} \quad \text{in V/m/s}^2. \tag{2.9}$$

With  $\rho$  the density of water in kg/m³, c the sound speed of water in m/s and f the frequency in Hz.

Or in in terms of sensitivity levels in decibels:

$$M_a = M_p + 20\log_{10}(\rho c) - 20\log_{10}(2\pi f)$$
 (2.10)

### 2.7.1.1 Water coupling aspect of a vector sensor

The operational frequency range of a vector sensor is limited by the accelerometer's specification and the ability of the sphere to follow the particle motion of the sound field. This is a function of the acoustic wavelength relative to the physical size of the sensor. Also the way the device is deployed and restrained or suspended in the field affects the ability to follow the particle motion of interest.

Due to the buoyancy for the non-unity specific gravity of the vector sensor, the measured particle motion can be expected to deviate from the actual particle motion field quantity [4] according to the equation:

$$\frac{v_S}{v_{inc}} = \left(\frac{3\rho_W}{\rho_W + 2\rho_S}\right) \tag{2.11}$$

where  $\rho_w$  is the density of the water and  $\rho_s$  is the density of the sensor in kg/m³.

A negatively buoyant sensor is less sensitive to particle motion than a neutrally buoyant sensor, due to the additional loading effects of the water. On the other hand a positively buoyant sensor would be more sensitive but impractical. The frequency response amounts to a calibration offset depending on the specific gravity. As frequency increases, all responses decrease in magnitude as a consequence of the spatial integration of the acoustic field over the sensor body: the acoustic size of the sensor acts as a low-pass filter, see Figure 2.4. Usually, the largest dimension of the overall device should be kept smaller than one tenth of the shortest wavelength of interest. Figure 2.4 shows that the coupling effect to water is only significant if the sensor is far from neutrally buoyant or if the dimension of the sensor is in the same order of magnitude as the acoustic wavelength.

In view of the present VHS-100 sensor with a specific gravity of 1.2, the ratio of the sensor motion in the direction of propagation  $(v_s)$ , normalized by the fluid motion in the absence of the sensor  $(v_{inc})$  equals 0.88. Due to this negatively buoyance effect a maximum amplitude deviation of 1 dB is expected. For other vector sensors with a higher specific gravity, like the M20 sensor, the buoyancy effect needs to be

accounted for in the dry calibration, see Section 3.1. It is automatically accounted for in the wet calibration, see Section 3.3. For the M20 sensor the buoyancy effect is expected to be 4 dB.

The low-pass filter effect is expected for the VHS-100 sensor. Its diameter d equals 0.09 m and the upper frequency limit is specified at

4 kHz. This results in a wavelength diameter ratio of 0.24 and a corresponding  $v_s/v_{inc}$  of 0.8 (-2 dB). So the maximum error of the measurement of the particle acceleration of the water is 1-2 dB.

 $v_s/v_{inc}$  is expected to deviate from the rigid sphere curve for materials with a finite impedance (high compliance) if the ratio between the wavelength and the diameter of the sensor becomes larger [4]. This indicates the importance of the choice of material type of the housing of a vector sensor.

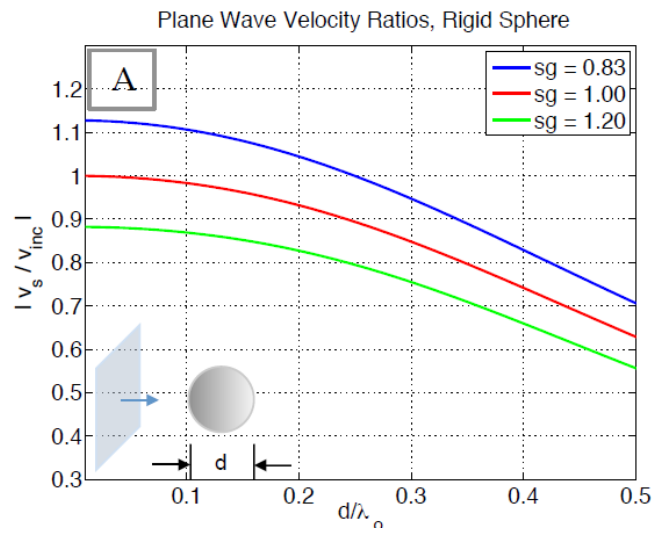


Figure 2.4 Plane wave responses of solid sensor body models in terms of  $v_s/v_{inc}$  as a function of the ratio of the sphere diameter over governing wavelength: analytical solution for rigid sphere response magnitude with varying specific gravities, taken from [4].

# 3 Calibration procedures

Although, currently no standard on the calibration of a vector sensor exists, various methods commonly used for the calibration of hydrophones are used as found in the literature. TNO made a selection and combination of procedures to follow in the TNO basin. This chapter gives an overview of calibration procedures that have been found in the literature. In the next chapter two calibration methods have been applied to the sensor.

#### 3.1 Shaker Method

For vector sensors which are based on the use of accelerometers, it is possible to calibrate these following existing ISO standards for calibration of accelerometers [7]. These methods rely on the use of a sinusoidal exciter or shaker and provide a calibration through comparison to a calibrated reference accelerometer. A large frequency range can be covered, also down to lower frequencies.

Potential phase differences become important when measuring the direction of a sound wave in terms of particle acceleration by combining the three individual accelerometer channels, see Chapter 6. The shaker method can also be used to phase calibrate the three accelerometer channels, by considering the cross-correlation of the acceleration signal in each orthogonal direction and the driving voltage fed to the shaker.

The shaker method does not include any loading and coupling aspects of water. It actually calibrates only the individual accelerometer components as mounted in the device. However, this coupling effect to water can be accounted for when required, see also Section 2.7.1.1.

## 3.2 Pressure gradient method

Sound particle acceleration can be determined from the difference of two pressure measurements made at different locations in space; see eq. (3.1).

$$a = -\frac{1}{\rho}\nabla p \tag{3.1}$$

This can be done with a pair of phase calibrated hydrophones with a fixed spacing  $(\Delta)$ .

This method only works if the hydrophone spacing is smaller than half the minimal wavelength of interest:

$$\Delta \le \frac{\lambda_{min}}{2} \tag{3.2}$$

So, if the particle motion needs to be derived up to 4 kHz, the required spacing  $\Delta$  has an upper limit of 18.8 cm.

In the calculation of gradients it is critical that the phase of the pressure signal is not be discarded, since the phase can add gradient contributions. Therefore, a phase calibration of the hydrophone pairs is also required. In [8] a procedure for a phase calibration is given.

#### 3.3 Free-Field Comparison method

The free-field comparison method relies on the defined relationship between sound pressure and particle velocity and therefore requires a free field plane wave field (travelling wave). This field condition however sets limits to the lower frequency range for which the calibration procedure is valid. When calibrations are performed in a semi-anechoic tank, the finite dimensions of the tank determine the lower frequency limit for which the free-field condition is approximated.

The reference hydrophone, projector and vector sensor are preferably positioned mid-water column. The reference centers were arranged in-line; see Figure 3.1. The distance between the projector and vector sensor and the projector and the hydrophone was fixed to 1 m.



Figure 3.1 Line-up of the reference hydrophone, projector and vector sensor.

Two types of signals were recorded during the calibration:

- Swept sine from 100 Hz 4 kHz;
- Tone-burst signal (chirp) signal with 5 ms pulse width.

To calculate the sensitivity of the vector sensor from the reference hydrophone, the hydrophone and particle motion need to be in the far-field at free-field conditions. If these conditions are fulfilled the sensitivity to acceleration of the vector sensor  $M_a$  in dB re  $1V/\mu m/s^2$  equals:

$$M_a = L_{V,pm} - L_{p,ref} + 20 \log_{10}(\rho c) - 20 \log_{10}(2\pi f)$$
(3.3)

with,

 $L_{V,pm}$  the voltage level of the Vector sensor in dB re 1 V<sub>rms</sub>.

 $L_{p,ref}$  the sound pressure level of the reference hydrophone in dB re 1  $\mu$ Pa.

 $\rho$  the density of the medium in kg/m<sup>3</sup>.

c the speed of sound in the medium in m/s.

f the frequency in Hz.

Also the sensitivity of the vector sensor to sound pressure  $M_p$  in dB re 1V/ $\mu$ Pa can be derived from the reference hydrophone:

$$M_p = L_{V,p} - L_{p,ref} \tag{3.4}$$

with,

 $L_{V,p}$  the voltage level of the pressure channel in dB re 1 V<sub>rms</sub>.

#### 3.3.1 Far-field condition check

In the comparison method [5] a reference hydrophone with a known frequency dependent sensitivity is positioned close to the vector sensor and a projector. If the projector behaves like a monopole source, and the radiated sound waves behaves like a plane wave, propagating under free-field conditions, the impedance (ratio of sound pressure over particle velocity) at a certain distance from the source is known [9]:

$$Z(r) = \rho c \frac{jkr}{1+jkr} \tag{3.5}$$

with,

 $\rho$  the density of water in kg/m<sup>3</sup>.

c the speed of sound in water in m/s.

k the wavenumber in m<sup>-1</sup>.

r distance between source and receiver.

The product of kr is known as the Helmholtz number which is proportional to the number of wavelengths that fit within distance r:

$$kr = \frac{2\pi}{\lambda}r = \frac{2\pi f}{c}r\tag{3.6}$$

The impedance at a certain distance from the source as a function of kr is plotted in Figure 3.2.

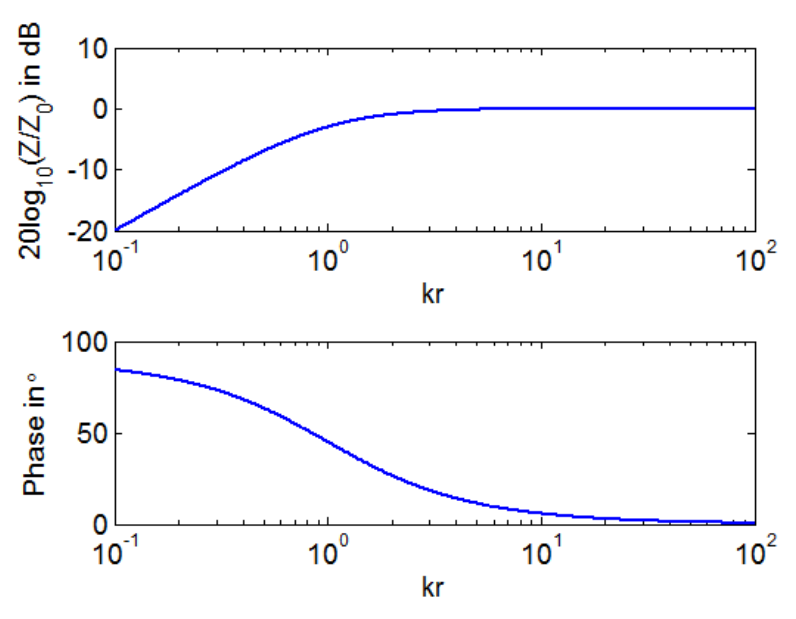


Figure 3.2 Absolute value and phase of the impedance normalized to the specific impedance  $Z_0$  ( $\rho_0 c_0$ ) of water as a function of Helmholtz number kr.

For kr << 1 there are a small number of wavelength between source and receiver. The impedance is much smaller than the specific impedance and also becomes reactive (90° phase angle). The impedance is governed by the local moving of the mass of the surrounding water.

For kr >> 1 many wavelengths fit between the source and the receiver. This condition is obtained a large distance and/or a high frequency. Under this condition the sound pressure and particle motion are in phase (0° phase angle) and the impedance equals  $\rho c$ . The receiver is then located in the far-field.

In order to have a far-field condition, a calibration distance of 1 m seems appropriate for a frequency range between 500 Hz and 4 kHz.

#### 3.3.2 Free-field condition check

For a vector sensor calibration under free-field conditions the dimensions of the semi-anechoic basin are a limitation towards lower frequencies. When wavelengths are too large the reflection from the water surface and the side walls will affect the acoustic signal at the receiver position and consequently violate the free-field conditions.

One way to overcome this limitation is to send a tone burst signal to the projector. The time selection of a tone burst in reflecting water tank measurements (timegating) can provide conditions for free wave propagation, because reflections are absent at a time interval no longer than the reflected signal time delay. It is possible to form a free field for only a short time, before the arrival of the first reflection at the receiver point; see Figure 3.3. This makes the method unsuitable for lower frequencies.

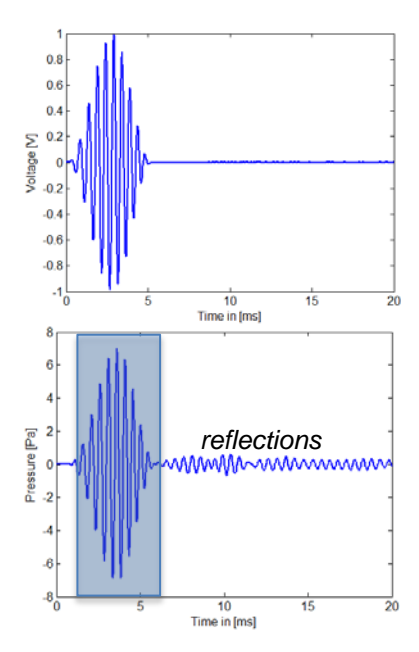


Figure 3.3 Example of a burst sine (upper, 2 kHz, 5 ms). This pulse is send to the projector and received by the hydrophone (lower). By time-gating reflections are removed.

#### 3.4 Self-noise

The self-noise of the vector sensor can be determined from the measured voltage levels. A very quiet environment with negligible ambient noise is required for this. The semi-anechoic basin should be installed on rubber blocks and therefore decoupled from the building in the higher frequency range. Self-noise levels, in

terms of acceleration levels, can be compared to the free-field Wenz curves as presented in Figure 2.1.

# 4 Calibration results vector sensor

In the former chapter several calibration procedures were discussed. Within the scope of the present SMO project two calibration methods were performed on two types of vector sensors, a low-frequency and a high-frequency method:

- the shaker table method from 20 Hz 1 kHz (Section 3.1);
- the comparison method in the TNO basin from 500 Hz 4 kHz (Section 3.3).

For all calibration measurements the vector sensor channels were connected to a multi-channel B&K LAN-XI data acquisition system.

#### 4.1 VHS-100

#### 4.1.1 Shaker Method

The vector sensor was put onto an electro dynamic shaker, without the suspension system, see left photo of Figure 4.1. If the resonance frequency of the vector sensor's suspension needs to be measured the sensor should be connected to the shaker in its suspension cage. A calibrated reference accelerometer (B&K 4517-002) was mounted to the outer shell of the sphere by beeswax. For each main direction the sphere and reference accelerometer were repositioned. From the transfer function from reference accelerometer to the vector sensor accelerometer voltage in the relevant direction, the sensitivity can be derived. The vector sensor was excited by the shaker with a swept-sine from 10 Hz - 10 kHz. Both amplitude and phase calibration were performed.







Figure 4.1 Vector sensor installed on an electro dynamic shaker, without the suspension system (left) and suspended in a cage in the center and on the right. For the calibration the vector sensor was not suspended in the cage.

#### 4.1.1.1 Amplitude calibration

A comparison between the sensitivity following from the shaker method and the specified sensitivity are plotted in Figure 4.2 for all orthogonal directions. The measurement results match the specifications well up to a frequency of 1 kHz. For higher frequencies the calculated sensitivities of the accelerometers drop-off. This effect can be explained by considering the measured acceleration levels of the outer shell and the inside of the vector sensor, see Figure 4.3. Whereas the outer shell acceleration levels stay more or less constant, the internal acceleration levels decrease for frequencies beyond 1 kHz. At these frequencies the external and internal accelerometers signals are not in-phase anymore. This effect can be used

to identify at which frequency the resonant behavior of the sphere starts and prevents the vibrational energy from entering the base of the sphere. Therefore, an alternative method is required to calibrate the vector sensor for higher frequencies in which the water coupling is also taken into account.

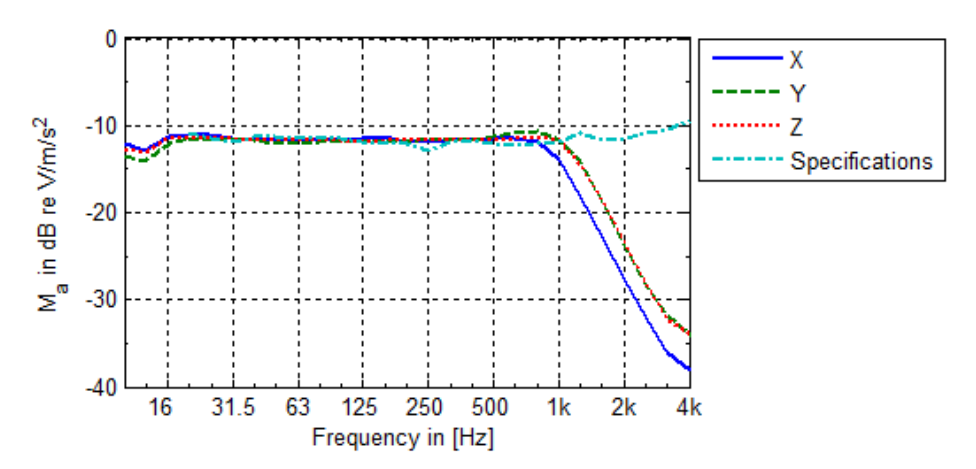


Figure 4.2 Sensitivities of the VHS-100 Vector sensor to acceleration in various directions a function of frequency, according to the specifications and obtained from the shaker experiments.

Figure 4.3 gives the acceleration levels of the reference accelerometer on the shell and the internal accelerometer of the vector sensor.

Besides the excited direction, Figure 4.4 shows the response of the other 2 channels in the orthogonal directions, in which direction the vector sensor was not excited. The acceleration levels are much lower, but the excitation spectrum is visible on these channels as a results of some cross-talk between the channels.

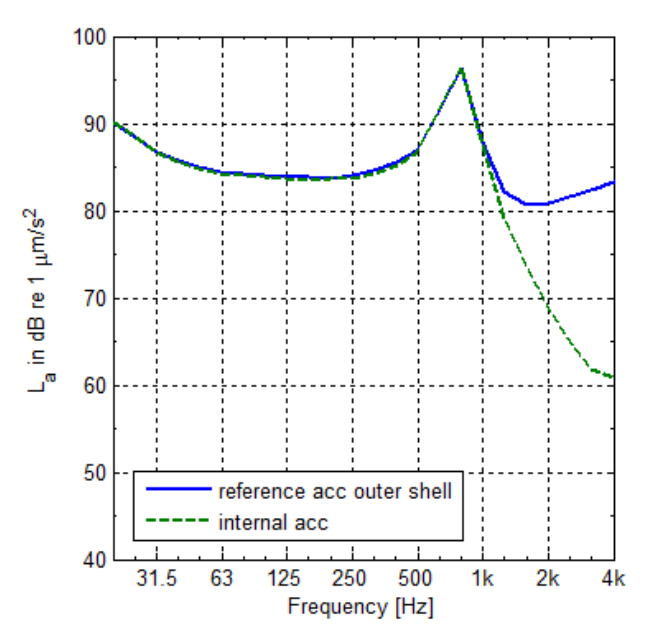


Figure 4.3 Acceleration levels of the vector sensor in vertical direction and the reference accelerometer on the outer shell of the vector sensor housing, when both excited by the same swept-sine signal (10 Hz-4 kHz).

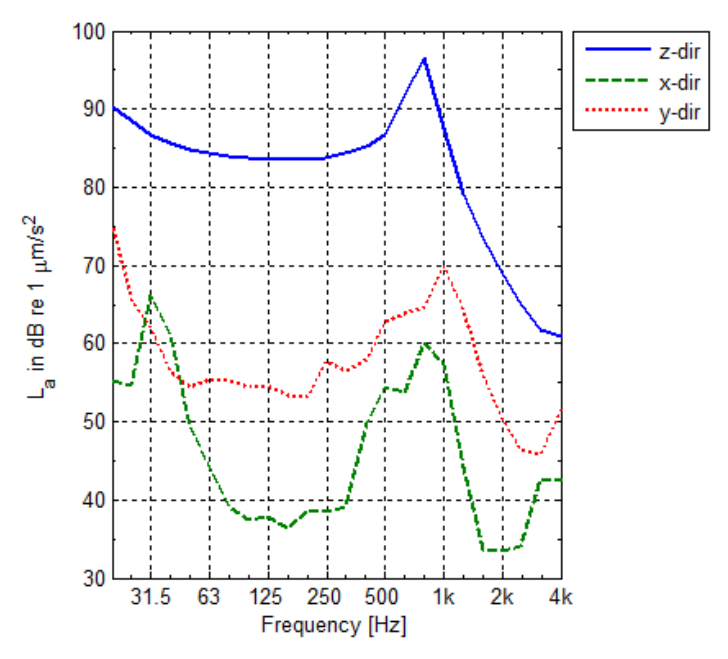


Figure 4.4 Acceleration levels of the VHS-100 vector sensor in all three orthogonal directions in third-octave bands. The z-direction was oriented in line with the excitation force of the shaker.

#### 4.1.1.2 Phase calibration

By considering the cross-correlation between the driving signal sent to the shaker and the acceleration signals, the phase between the acceleration channels can be checked, see Figure 4.5. If the accelerometers do not respond in phase, the accuracy of the measurement of a directional acceleration vector will be decreased. Figure 4.5 shows that all accelerometer channels act in phase. The phase jump at 60 Hz is probably an effect in the electronics of the signal conditioner or preamplifier, but occurs on all channels.

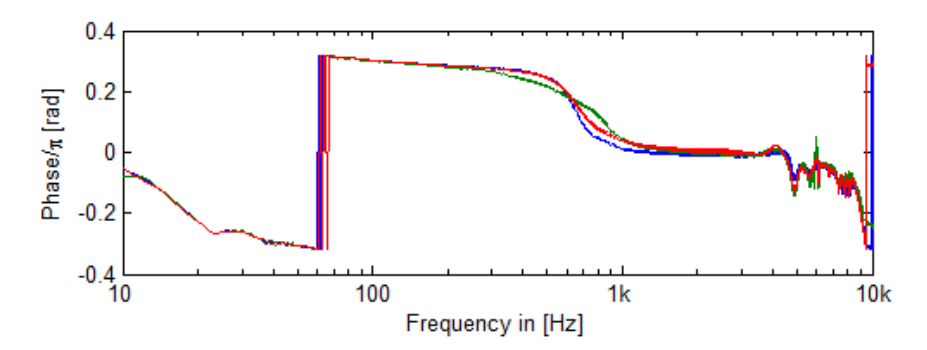


Figure 4.5 Comparison of the phase of the three transfer functions of particle motion acceleration over driving voltage of the shaker as a function of frequency ( $\Delta f = 1 \text{ Hz}$ ).

## 4.1.2 Free field propagation in TNO basin

As discussed a vector sensor can be calibrated by a reference hydrophone by making use of the relationship between sound pressure and particle velocity for a propagating plane wave under free-field condition (eq. 2.2).

The attenuation of a plane wave with increasing distance under free-field condition follows the 1/r law. To check from which frequency a plane wave field can be achieved in the TNO basin an additional experiment was done.

An ITC 1001 projector was deployed in the center of the TNO basin at 4 m depth. A B&K reference hydrophone was deployed at the same depth at a distance varying between 0.5 - 1.5 m.

For each set-up two signals were send to the ITC 1001 by a AE Techron amplifier:

- a swept sine (100 Hz 10 kHz);
- a burst sine of 5 ms at 500 Hz, 1 kHz, 2 kHz, 3 kHz and 4 kHz.

The sound pressure levels on the hydrophone were determined for the various signals and hydrophone/projector distances.

Figure 4.6 shows the attenuation of the sound pressure level measured on the hydrophone with increasing distance between projector and hydrophone. It shows that for continuous sweeps the 1/r law is approached for frequencies beyond 2 kHz. For 5 ms sine burst signals for frequencies down to 500 Hz free field propagation can be approached when time gating the hydrophone signals. For the TNO basin a 5 ms burst signal is required if the transducers are deployed at the center of the water column (depth of 4 m). When the transducers are deployed at 4 m depth, the minimal time delay of the reflecting wave equals  $2 \cdot 4/1500 = 5 \, ms$ .

The measurements were repeated with the interchanged projector and hydrophone positions to check monopole directivity of the projector. The ITC-1001 seems to act as a monopole source in the frequency range of interest.

In Section 3.3.1 is already shown that at a distance of 1 m from a monopole source, the hydrophone is located in the far-field. Figure 4.6 shows that at this condition also the free-field requirement is fulfilled for a large part of the frequency range dependent on the type of source signal.

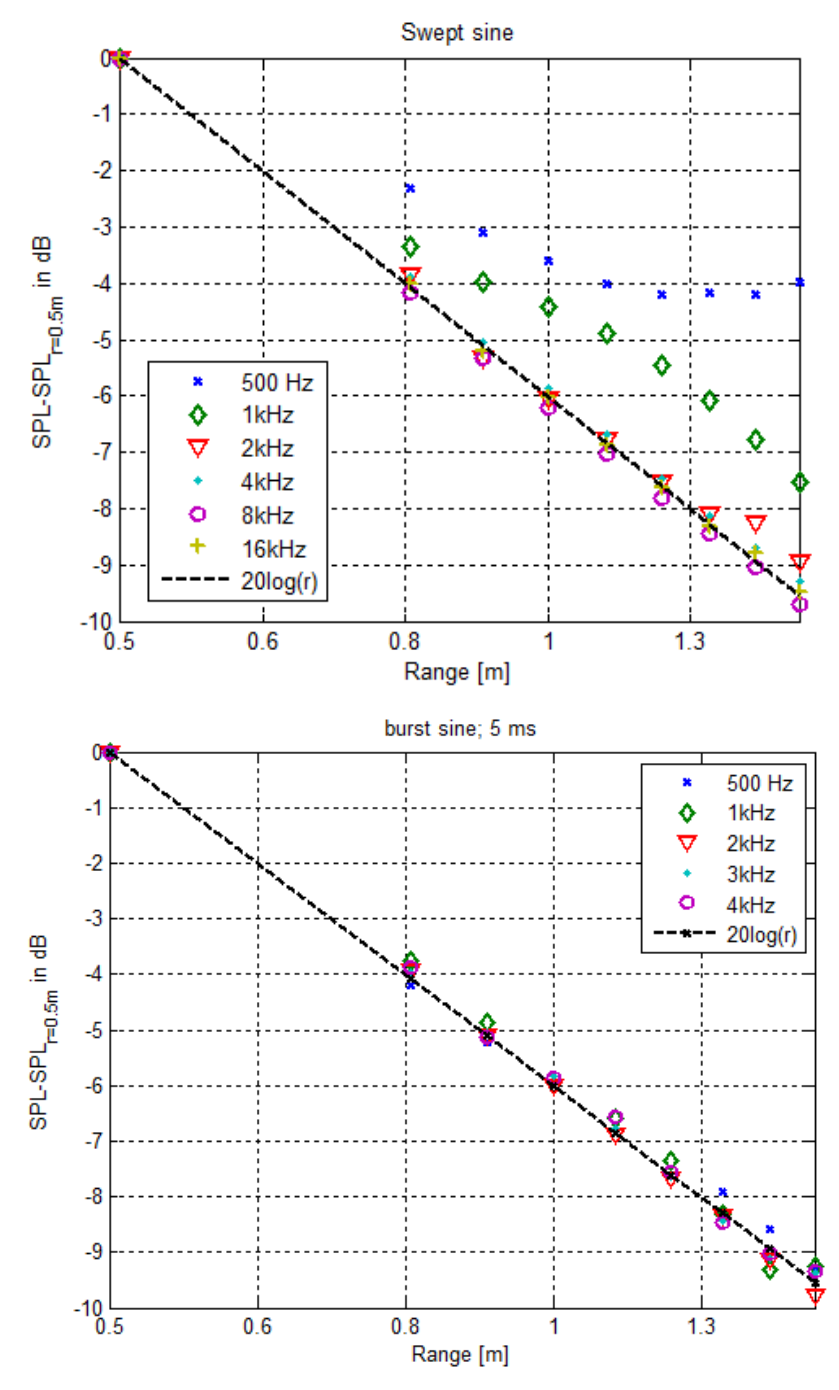


Figure 4.6 Attenuation of the sound pressure level on the hydrophone with increasing distance between the projector and the hydrophone, for various frequencies. The upper plot shows the attenuation for a continuous swept sine signal, the lower a 5 ms burst sine.

## 4.1.3 Comparison method

Figure 4.7 shows the results of the comparison method with application of the continuous swept-sine and the short burst sine signals. For higher frequencies, for both types of signals the results of the comparison method match the specified sensitivities well. For lower frequencies below 1 kHz, the sound field produced by the swept-sine signal does not result in a free-field condition in the TNO basin anymore. Consequently the sensitivities deviate from the specification. By using the

time-gating technique on the 5 ms burst-sine signals, the frequency range in which the comparison method works for the TNO basin can be lowered to 500 Hz.

Figure 4.7 also shows the sensitivity resulting from the shaker test. The mismatch with the specifications beyond 1 kHz does not seem to occur for the comparison method, during which the vector sensor is in contact with water. The possible physical explanation for this phenomena is a better match of the specific impedance of epoxy resin of the vector sensor's housing with water than with air.

At low and mid-frequencies the results of the shaker test match the results of the comparison test. Apparently the effects of the coupling to water, see Section 2.7.1.1, are negligible and the shaker results do not need a correction for these coupling effects for the VHS-100 sensor.

Both applied calibration methods seem to be complementary. Whereas the shaker method is not suitable for higher frequencies, the comparison method in the TNO basin is not suitable for lower frequencies. In the mid-frequency section the results of both methods overlap.

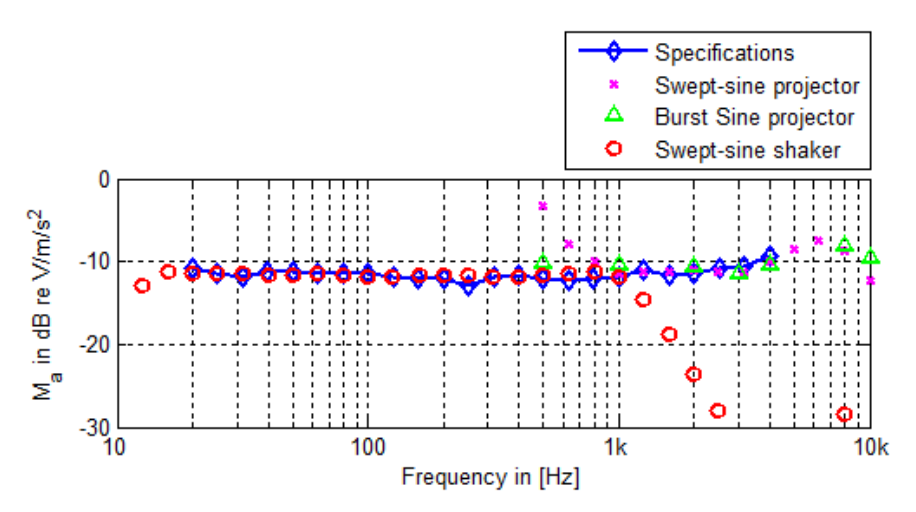


Figure 4.7 Sensitivity of the accelerometer of the vector sensor determined from the shaker method (swept-sine shaker table) and the comparison method (swept-sine projector and burst-sine projector). Also the specified sensitivity are shown.

Using the comparison method, the sound pressure channel of the vector sensor has also been calibrated and compared with the specifications down to 500 Hz; see Figure 4.8.

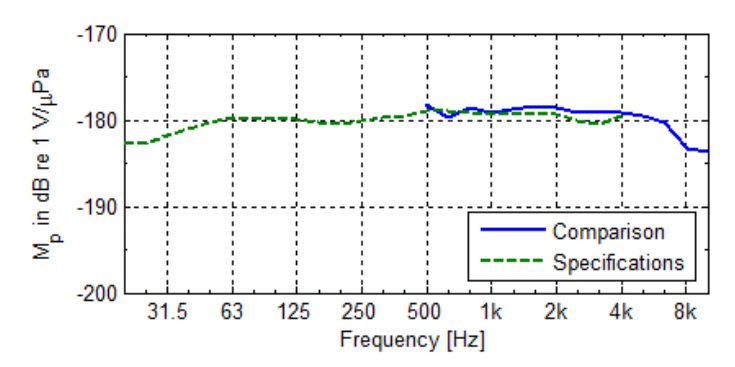


Figure 4.8 Sensitivities of the sound pressure channel to pressure according to the specifications and obtained from the comparison method.

#### 4.1.4 Self-noise levels

The self-noise is measured using the method described in Section 3.4.

#### 4.1.4.1 Underwater

Figure 4.9 shows the ambient sound particle acceleration levels at sea, derived from the sound pressure levels of the Wenz curves in third-octave bands. For frequencies above 500 Hz the Wenz curves describe the ambient sound levels in the oceans induced by the waves and the wind conditions. Also the measured ambient acceleration levels in the TNO basin are shown in the figure. It shows that for higher frequencies the self-noise level is 10 dB below the acceleration levels at sea-state 1. The main pumps of the basin were turned off during the measurements, but still some tones caused by other installations are present in the spectrum. The background noise level at lower frequencies is governed by external sources and do therefore not represent the sensor's self-noise floor. When the high-frequency line for the self-noise floor is extrapolated towards lower frequencies it is expected close to sea-state 1 at 25 Hz.

The measured acceleration levels can be converted to plane wave sound pressure levels; see Figure 4.10. This leads to similar conclusions. Also the ambient noise of the pressure channel of the vector sensor is shown in this figure. The noise floor of the sensor is about 20 dB higher than for a B&K 8106 hydrophone with comparable sensitivity.

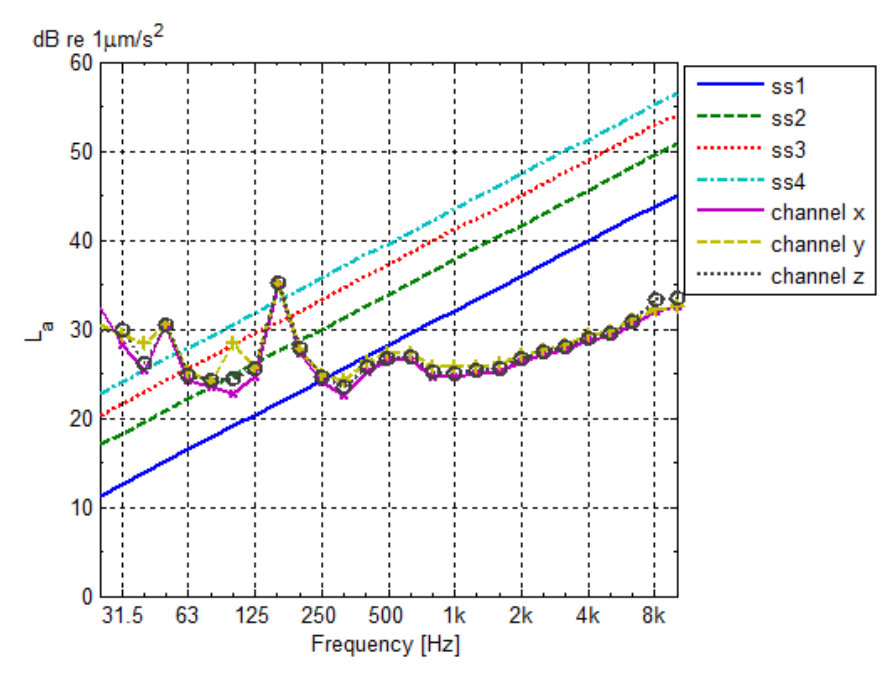


Figure 4.9 Ambient acceleration levels at sea for various sea states, derived from the sound pressure levels following the Wenz curves assuming free-field condition. The ambient acceleration levels as measured in the TNO basin are also shown in this figure.

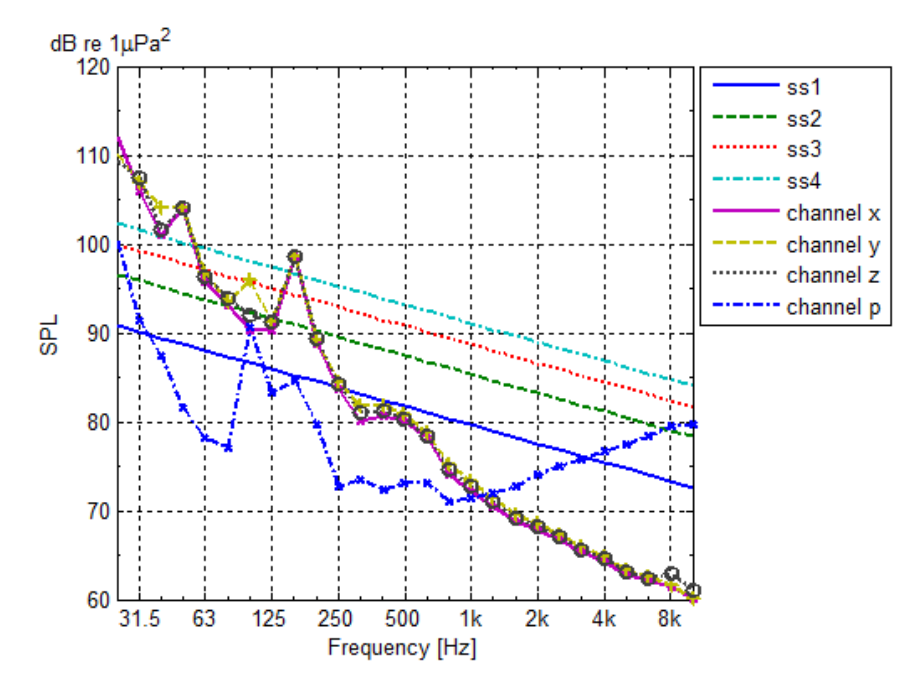


Figure 4.10 Ambient sound pressure at sea for various sea states following the Wenz curves assuming free-field condition. The ambient sound pressure levels and acceleration levels as derived from the measured ambient acceleration levels (assuming free-field condition) are also shown.

#### 4.1.5 Complex impedance check

Now that all accelerometers and sound pressure channels have been calibrated, the complex impedance at 1 m from the projector can be measured by the vector sensor, and compared to the theoretical value of eq. (3.5); see Figure 4.11.

This complex ratio p/u was determined from the ratio of the cross power spectral density of p and  $a(G_{pa})$  over the power spectral density  $(G_{pp})$ :

$$\frac{p(\omega)}{u(\omega)} = \frac{1}{i.\omega} \frac{G_{pp}(\omega)}{G_{nq}(\omega)} \tag{4.1}$$

The measurement results match the theoretical results quite well for Helmholtz numbers down to 2. At high Helmholtz numbers, for frequencies beyond 4 kHz, the measured impedance starts to deviate. This can be explained by the sensitivities of both the pressure and accelerometer channels which are deviating from the nominal sensitivity and cannot be considered to be frequency-independent anymore. For Figure 4.11 the nominal sensitivities were taken.

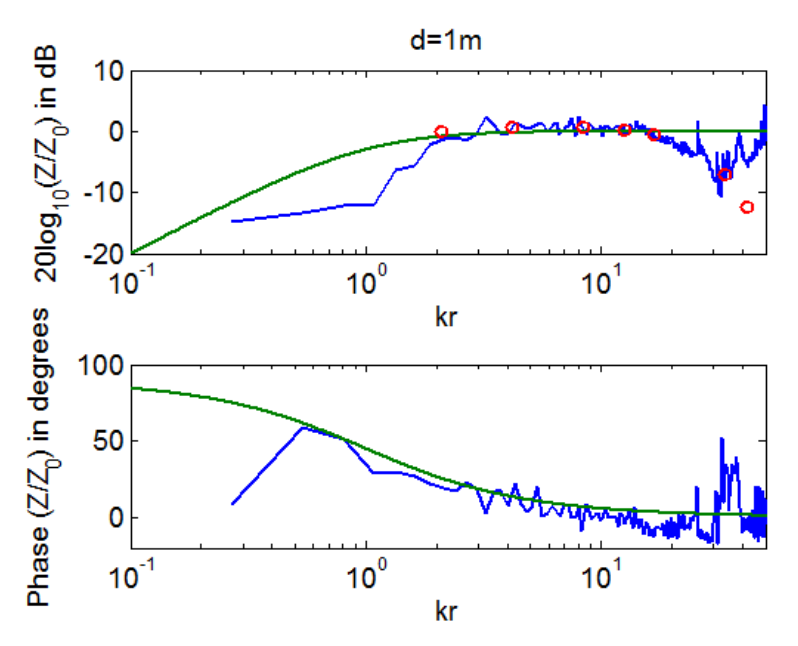


Figure 4.11 Theoretical (blue lines for swept-sine and red dots for burst-sine signals) absolute value and phase of the impedance normalized to the specific impedance  $Z_0$  (pc) of water as a function of Helmholtz number kr.

#### 4.2 M20 sensor

The M20 sensor is much larger and heavier than the VHS-100 sensor and also the suspension is very different, see Figure 4.12. The sensor is deployed from a rope on the lifting eye, so the system behaves like a pendulum. No recommendations on the length of the rope are provided. To study the effect of the length of the deployment rope on the sensor performance, the length was varied during calibration: 0.25 m and 1 m.



Figure 4.12 Overview of the M20 sensor with the lifting eye on the top.

## 4.2.1 Shaker Method

Figure 4.13 shows the measurement set-up with the M20 connected to an electro-dynamic shaker. The reference accelerometer is mounted on top of the housing. The measured sensitivity of the M20 to acceleration in various directions is shown in Figure 4.14. Due to high electrical self-noise levels of the sensor below 100 Hz, the sensitivity could not be determined for low frequencies. Increasing the excitation level of the shaker to overcome this electrical noise resulted in clipping of the accelerometer signal. The response curve as shown in Figure 4.14 is very typical for the M20 [10]. At low frequencies the sensitivity to acceleration is more or less independent from frequency. The sensitivity peaks at the mechanical resonance of the accelerometer then decreases by 14 dB per octave above resonance. Oil is added inside the housing of this sensor to dampen the mass' movement and smooth out the resonant peak.



Figure 4.13 M20 Vector sensor installed on an electro dynamic shaker in various directions.

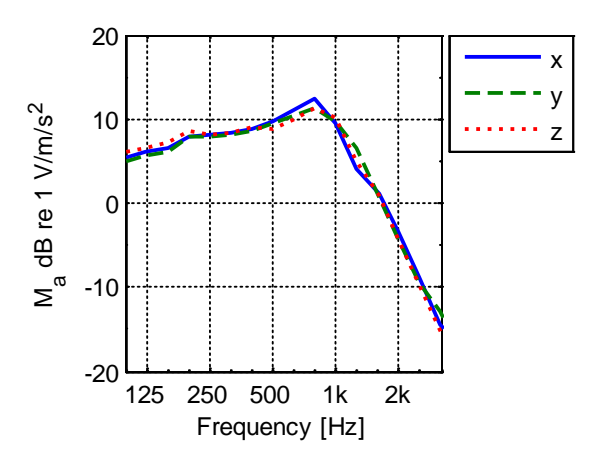


Figure 4.14 Sensitivities of the VHS-100 Vector sensor to acceleration in V/m/s² in various directions a function of frequency obtained from the shaker experiments.

Figure 4.15 shows the response in x and y direction while the sensor is excited in z- direction only. The acceleration levels in these directions are much lower, but the excitation spectrum is visible on these channels as a results of cross-talk.

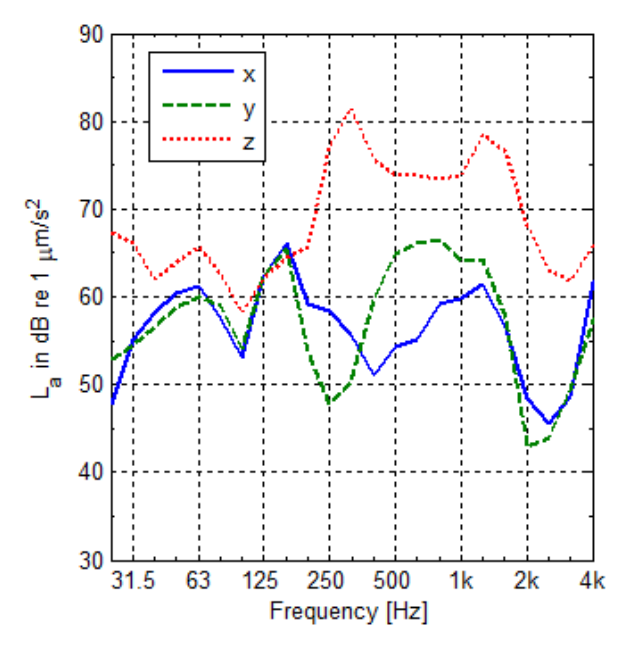


Figure 4.15 Acceleration levels of the VHS-100 Vector sensor in all three orthogonal directions in third-octave bands. The z-direction was oriented in line with the excitation force of the shaker.

## 4.2.2 Comparison method

The M20 was deployed 1 m from the projector at 4 m depth; see Figure 4.16. The sensor was connected to a submerged stiff rod by a rope of respectively 0.25 m and 1 m length. The x and y axes were oriented in the horizontal plane of the projector. The z-axis of this sensor is always oriented in vertical direction.

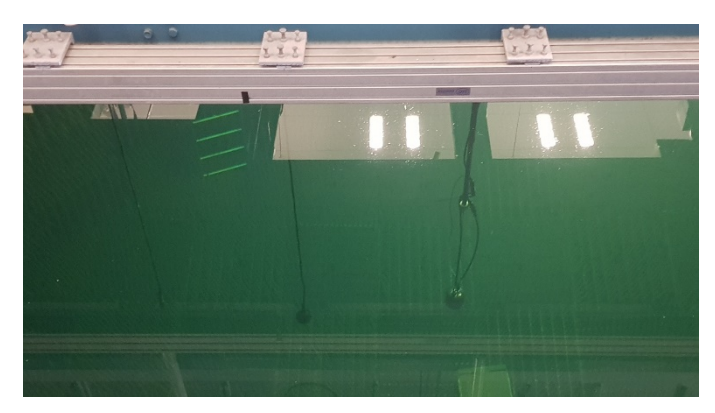


Figure 4.16 Reference hydrophone poisoned 1 m to the left of the ITC-1001 projector and the M20 at 1 m to the right.

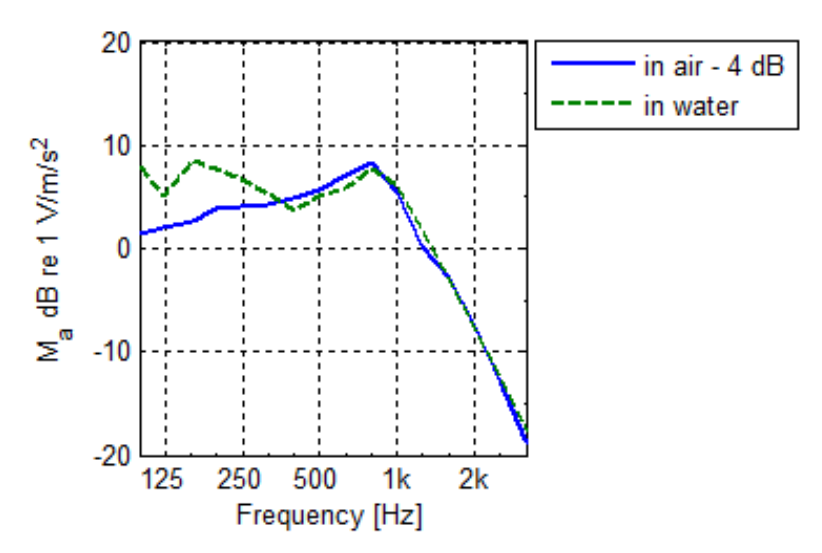


Figure 4.17 Sensitivity of the accelerometer of the vector sensor determined from the shaker method (in air) and the comparison method (in water).

Figure 4.17 shows the sensitivity to acceleration according to the comparison method (wet calibration) and the shaker method (dry calibration). After correction for the buoyance effect, following eq. (2.11), the correspondence is very good. The negatively buoyant M20 is 4 dB less sensitive to acceleration in water than in air. The sensitivities to acceleration in water shown in Figure 4.17 were measured with a suspension rope length of 1 m. Results of a shorter rope length of 0.25 m show the same results, which implies that the rope length within the considered range is not critical for the sensitivity of the M20 to particle acceleration in water. Compared to the results of the VHS-100 sensor in the former section, the results of the comparison and shaker method match up to much higher frequencies. This is because the housing of the M20 is stiff and heavy and the sensor has a first body resonance at about 4 kHz [10].

Figure 4.18 shows the phase angle of the ratio of acceleration response in x and y direction to the driving voltage sent to the transducer as a function for frequency. The response seems to be slightly out of phase. This is something to take into account when the M20 is used for getting the direction of arrival of a sound wave, e.g. by polarization algorithms; see Chapter 6.

Within this respect also the phase relationship of the ration p/u under free-field conditions is important, it should converge to 0 degrees (p and u in phase) at high frequencies under free-field conditions. Figure 4.19 shows this is not the case. The phase mismatch is frequency dependent and is large, over 153 degrees at 3 kHz. This implies that a phase correction is required on the acceleration channels if the M20 is to be used for directional estimation using acoustic pressure.

Figure 4.20 shows the hydrophone channel sensitivity as a function of frequency. It shows a very frequency dependent behavior.

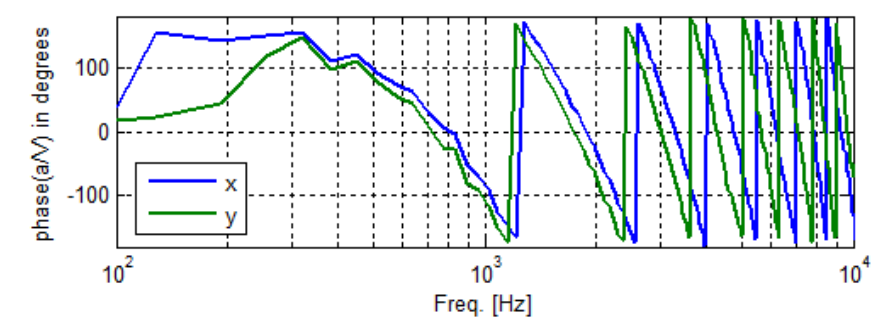


Figure 4.18 Phase angle of driving voltage a/V in x and y direction ( $\Delta f= 1 \text{ Hz}$ ).

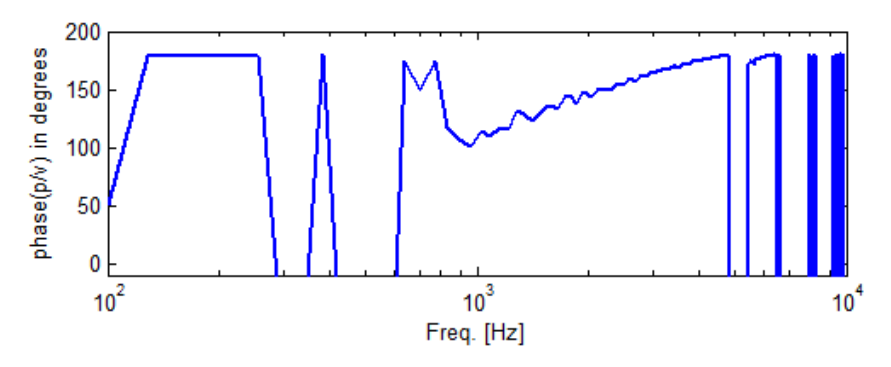


Figure 4.19 Phase angle of the ration p/v as a function of frequency ( $\Delta f = 1$  Hz) for the M20.

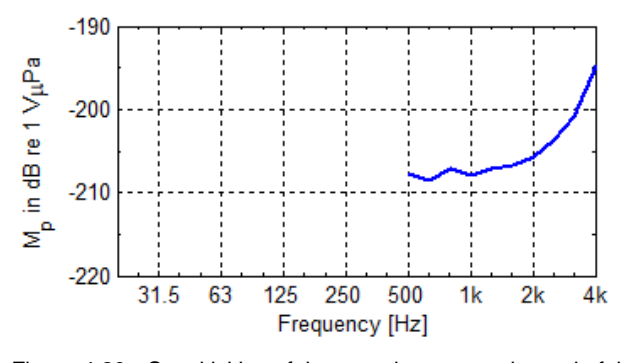


Figure 4.20  $\,$  Sensitivities of the sound pressure channel of the M20.

#### 4.2.3 Self-noise levels

Figure 4.21 shows that the self-noise levels on the acceleration channels are below the levels for sea state 1. The self-noise level of the hydrophone channel was very high due to electronic interference on the sound pressure channel and is not shown in Figure 4.21.

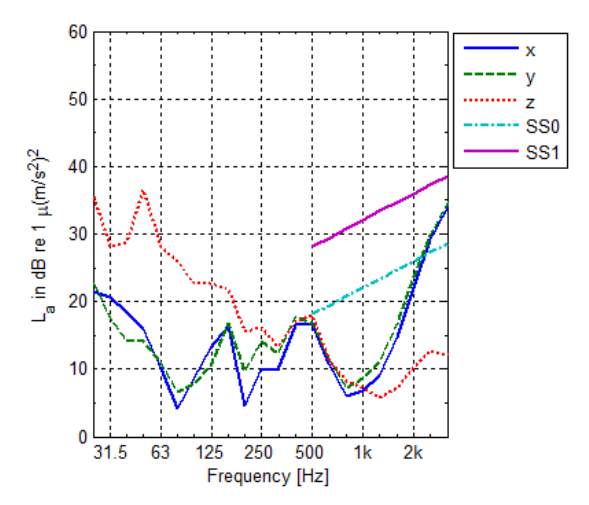


Figure 4.21 Ambient levels of the accelerations as measured in the TNO basin (averaged over 30 s) with the Wenz curves for various sea states. In the figure the SPLs for various sea states have been converted to acceleration levels assuming plane-wave conditions.

#### 4.3 Discussion

Two different types of vector sensors have been characterized following the designed measurement procedures. The sensors can be benchmarked.

Both sensors vary in size and weight. The VHS-100 weights about 0.5 kg in air and has a 9 cm diameter. The M20 weights almost 4 kg in air and has the shape of a cylinder, length of 17 cm and diameter 13 cm. However, the suspension cage of the VHS-100 is also 17 cm in diameter, so effectively the same amount of space is required.

The studied version of the M20 was much more sensitive to particle motion (10-15 dB) then the VHS-100. This in combination with a low self-noise levels on the accelerometer channels, makes the M20 suitable to monitor ambient levels. Due its sensitivity the tested M20 tends to clip at relatively low levels. This makes the sensor less suitable to record particle motion near loud sources like a pile driver.

The offset on the phase response on the various acceleration channels of the M20 and the sound pressure and acceleration response makes the sensor less suitable for the estimation of the directivity of sound waves. A proper phase calibration is required to match the phase of the signals. The phase characteristics of the VHS-100 are good and require no correction.

# 5 Field tests

#### 5.1 Introduction

After the calibration of the vector sensor in the laboratory, two field tests with the VHS-100 sensor were performed in different aquatic environments in Dutch waters. The field test reflect two use cases for industrial activities at sea resulting in underwater sound: seismic surveys and marine pile driving in shallow water.

The first campaign was performed in the Haringvliet in the Netherlands. The vector sensor was deployed at various depths and the source was positioned at various distances from the sensor.

The vector sensor was also put on the sediment, to study the performance of a vector sensor in the sediment. The ability to measure particle motion of the sediment is relevant for bio-acousticians, since a lot of fish and invertebrate species live close to or in the sediment. The vector sensor on the sediment can be subjected to excitation by other wave types in the sediment or at the water/sediment interface then only via the water-borne sound path. This makes the sensor potentially useful for studies in the field of the contribution of sediment and/or interface waves to the sound pressure and particle acceleration levels close to the sediment.

A second measurement campaign was performed in the North Sea during a pile-driving event. The sensor position was kept constant, but close to the sediment.

The results of these measurement campaigns have been published in reference [11]. In this reference also a comparison with a predicted sound particle acceleration by an acoustic model is presented. The main experiment results are summarized in this chapter.

## 5.2 Shallow Inland waterway

In November 2018 a field experiment was performed in a wide shallow inland waterway, the Haringvliet in the Netherlands. Local depth at the position of the sensor was 6-9 m. The vector sensor was placed at various receiver depths over the water column from a pier by different ways of deployment; see Figure 5.1. For the first deployment method the sensor was hung from a rope connected to a rod with and without a surface buoy on the water surface. The latter results in more wave induced motion of the sensor, typically in the lower frequency range. For the near sediment position the vector sensor was mounted on a box-like frame which was put on the sediment, Figure 5.2.

Finally, the sensor was taken out of its suspension cage and put into the muddy sediment with a random orientation and unknown coupling with the sediment. The unknown orientation is not a problem since the resultant particle motion vector is calculated.

A scaled airgun with 164 cm³ (10 in³) volume and 800 kPa (8 bar) operation pressure amplitude was used as a point source, see Figure 5.1. The airgun was moved out from the stationary sensor position by a boat from a range of 20 m up to

400 m. The depth of the source was 4 m. The water depth at the different source positions varied between 10 m and 18 m.

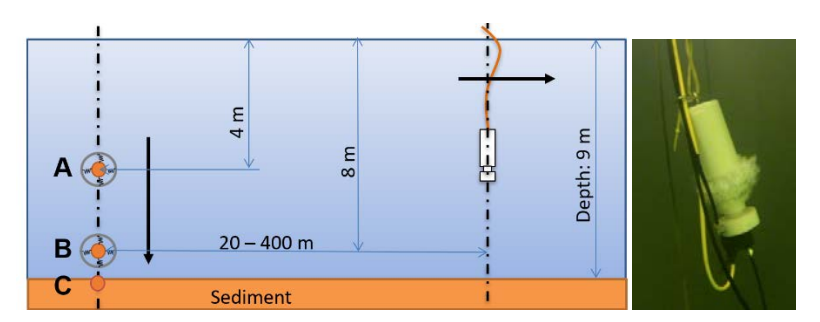


Figure 5.1 Experimental set-up of the vector sensor and airgun source in the shallow inland water environment.



Figure 5.2 Recovery of the vector sensor at the cage at the Haringvliet inland waterway.

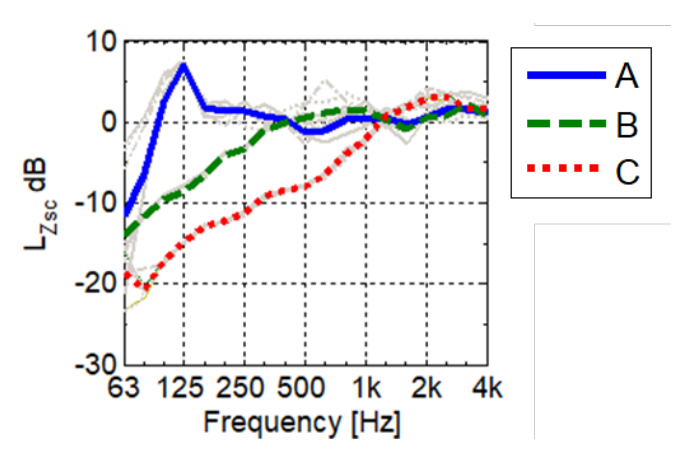


Figure 5.3 Measured scaled impedance in third-octave bands of various locations in the water-column (A: mid-water column, B: 80 cm above sediment) and in the sediment (C), averaged over series of 10 airgun shots per distance point. The gray lines indicate the result for each considered distance in a range of 20 m - 400 m.

For all airgun positions and vector sensor deployment depths the scaled-impedance  $L_{Z_{sc}}$  has been calculated, see Figure 5.3. It shows that  $L_{Z_{sc}}$  varies significantly with frequency and deployment depth, but variation with distance from the source is small.  $L_{Z_{sc}}(f)$  is shown to become small for low frequencies and to stabilize for

higher frequencies, where the source-receiver distance represents a larger number of acoustic wavelengths. The transition frequency depends on the receiver distance from water surface and seabed. Up to 15 dB difference in  $L_{Z_{sc}}(f)$  between the sensor at mid-water (4 m depth) and at near-seabed (7 m depth) are observed at 80 Hz, which is a variation in depth of only about 1/6 of the acoustic wavelength at this frequency. For higher frequencies from 500 Hz  $L_{Z_{sc}}$  approached 0 dB, which allows the conversion of u from p. The change in distance of the receiver from the reflecting water surface and the sediment, strongly affects the drop-off , resulting in a serious underestimation if u. The 6 dB overshoot of  $L_{Z_{sc}}$  at 125 Hz, which implies a 6 dB over estimation of u, is a result of the waveguide sound propagation in the shallow channel.

#### 5.3 North Sea

For the second field tests, the vector sensor was deployed from the sea surface at a depth of 20 m and at a distance of 750 m from a pile driver at the North Sea, see Figure 5.4. The diameter of the monopile was about 6.5 m. Due to the movement of the surface buoy and the connected vector sensor suspension cage induced by the surface waves, the self-noise floor was very high for frequencies below 50 Hz;, see also Figure 5.5. This is a result of the soft suspension system resulting in high wave induced oscillations in the low frequency range. For a better particle motion measurement in the lower frequency range, the vector sensor should have been mounted on a rig in the seabed.

For higher frequencies above 50 Hz the signal-to-noise ratios of the acceleration channels were high enough the calculate the scaled impedance  $L_{Z_{sc}}$ , which is presented in Figure 5.7. Again, the density of the water and the sound speed were measured by a CTD probe ( $\rho$  = 1022 kg/m³; c = 1480 m/s).

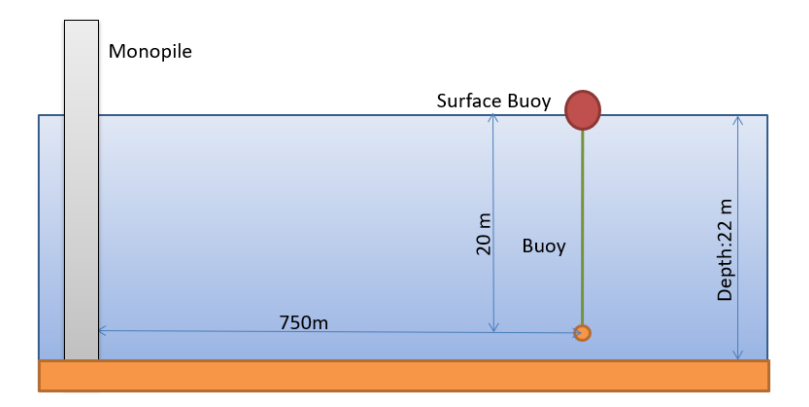


Figure 5.4 Experimental set-up of the vector sensor and pile driver source in the sea environment.

Figure 5.7 shows that  $L_{Z_{SC}}$  varies between -1 and 2 dB in the 63-4 kHz band, which indicates that the particle motion can be calculated following eq. (2.2) within 3 dB. In contrast to the point sources used in the former experiment, the monopile behaves as a line source. Therefore the reflected pile driving wave front behaves as a plane wave, which justifies the use the equations describing such a wave. It is remarkable that the particle motion at a position 2 m above the seabed is hardly affected by seabed reflections at low frequencies. At 63 Hz the offset of the receiver from the seabed is only 9% of the governing wavelength.

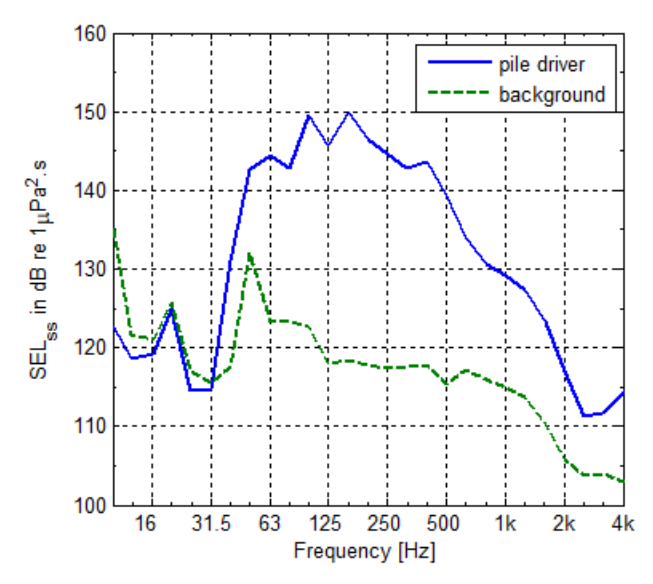


Figure 5.5 Sound exposure level of the piling signal (1.5 s integration time) and the exposure level of 1.5 s ambient sound, in third-octave bands.

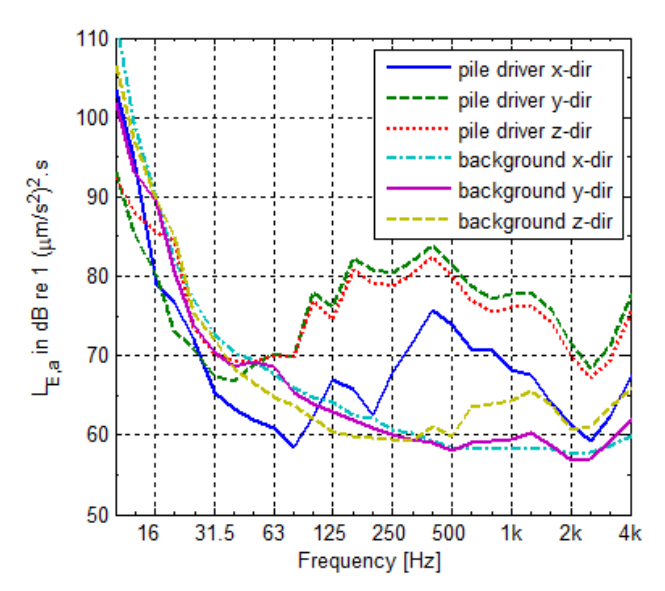


Figure 5.6 Sound particle acceleration level of the piling signal (1.5 s integration time and the exposure level of 1.5s ambient sound particle acceleration in various orthogonal directions, in third-octave bands.

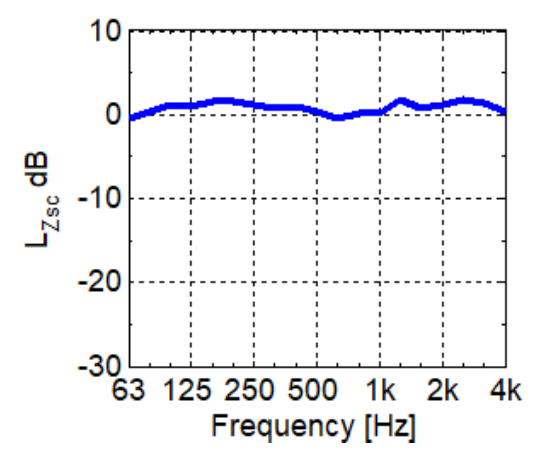


Figure 5.7 Measured scaled impedance in third-octave bands 2 m above the seabed at 750 m from a pile driver for one strike.

## 5.4 The effect of tidal flow on the background noise level

A vector sensor deployed at sea is subjected to tidal flow. This can affect the background noise level on the channels of the sensor. The depth of the vector sensor was measured by a co-located depth sensor (see Section 7.1.1 for more information about this logger). From this data it could be shown that within a 4 hour window the depth of the vector sensor varies between 20 m, when the line was vertically oriented in absence of tidal flow during dead tide, and about 10 m, when the tidal currents were strong; see Figure 5.8. This allows selection of a part of the ambient recording with and without tidal flow. Comparison of the sound pressure and acceleration levels of the various channels indicate the strong sensitivity of the acceleration signals to flow. The background noise levels of the acceleration channels are increased up to 15 dB.

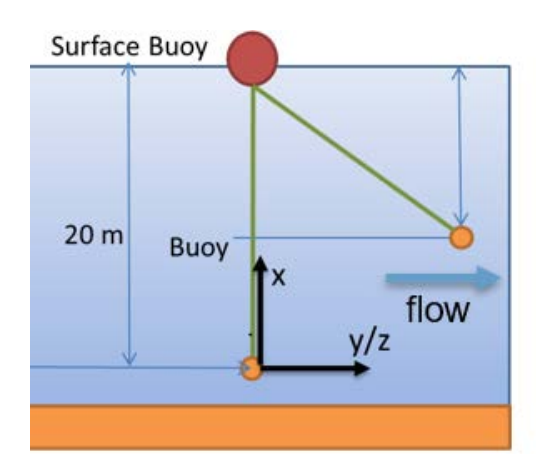


Figure 5.8 Overview of position of vector sensor on a line in tidal flows.

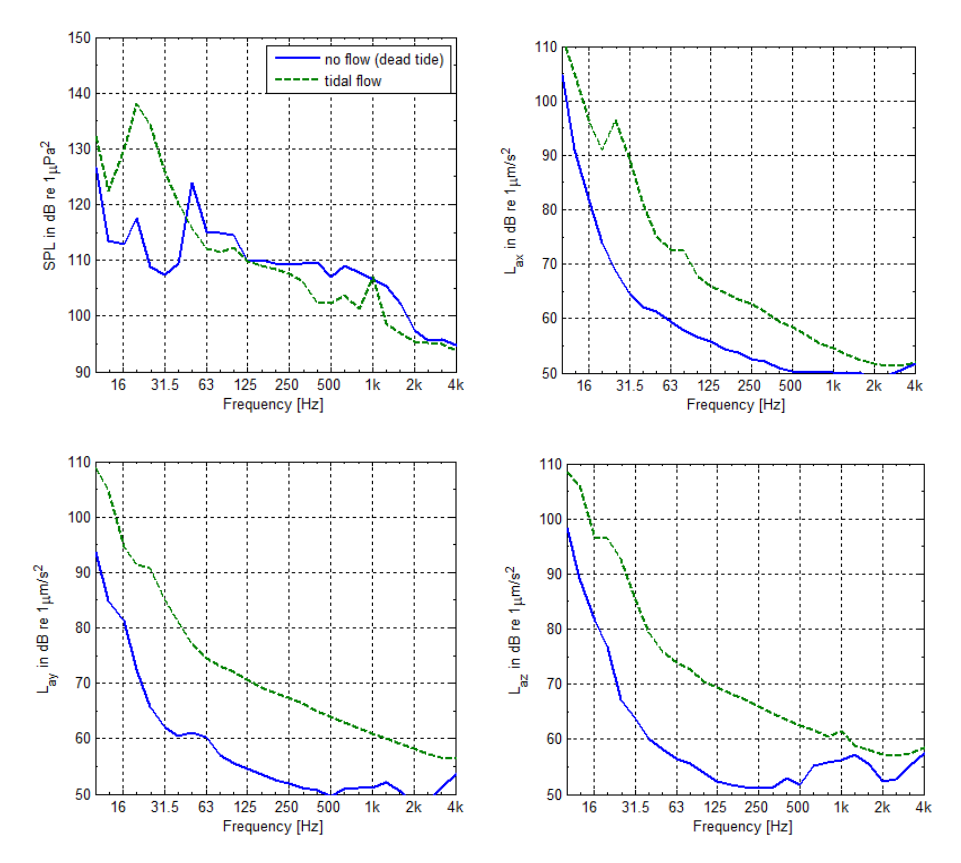


Figure 5.9 Effect of tidal flow along vector sensor on flow noise level of the sound pressure channel (top left) and the three acceleration channels of the vector sensor.

#### 5.5 Discussion

This chapter has shown first results from the field with the new vector sensor. Results are considered as satisfactory. It is shown that deploying a vector sensor from the surface on a float at sea, prevents measurements of particle motion in the for fish relevant lower frequency range. Also the importance of measuring the vector sensor's orientation is illustrated. These aspects should be taken into consideration for future measurement campaigns.

Experimental data on ambient sound levels and directional components of particle motion in different aquatic environments have been collected to study the conversion of sound pressure measured with a single hydrophone to particle motion assuming plane-wave conditions. The cases in shallow waters show that this conversion is subject to large errors for a point source for frequencies below 1 kHz. There are circumstances in which the level of particle motion is either higher or lower than predicted by the plane-wave relationship for a given sound pressure level, for example close to a source, in waveguides, or near boundaries. For these conditions, in absence of validated acoustic models, measurement of the particle motion with a dedicated sensor is required.

For a line source however, the calculated particle motion levels are within 2 dB from the measured levels in a broadband frequency range. This shows a good potential for obtaining an estimation of the particle motion from a single hydrophone reading for a line source for frequencies above cut-on frequency.

The scaled impedance metric is proposed as a convenient way to quantify the sound pressure – particle motion conversion as a function of range, frequency and depth. It varies significantly with receiver depth, but the variation with receiver distance from the source is much less.

Especially in shallow waters, the frequency region in which velocity/pressure ratio varies significantly can coincide with the frequency range of interest for bio-acoustic studies. Therefore a direct measurement of particle motion is necessary under these conditions.

The field tests described in this paper cover only a selection of relevant acoustic source types, aquatic environments and distances from the source. In order to define general recommendations on when to allow conversion of single hydrophone measurements to particle motion in bio-acoustic studies, more relevant cases need to be studied. But the results of the field tests described in this chapter illustrate that careful consideration is required when particle motion is derived from a single sound pressure measurement, especially for frequencies below or near the cut-on frequency.

Deployment of a vector sensor by a surface-buoy at sea is not advisable if particle acceleration measurements below 100 Hz are to be made. The self-noise due to the movement of the surface buoy is too high. Deployment on the seabed in a cage structure is preferred in this case.

It has been illustrated that a vector sensor can be used to measure particle motion in the sediment. This feature can be applied to study the particle motion of the sediment due to e.g. pile driving activities. The contribution of interface waves and compressional waves can be compared, or the contribution of the ground path to the particle motion of a response point close to the sediment.

# 6 Directionality of sound

The measurement of the sound particle acceleration in three orthogonal directions allows determination of the direction of a sound wave. The azimuth and vertical angle of a source, like a boat, can be determined by a so-called polarization analysis of particle motion measurements [13]. The particle motion values are input to eigenvalue/eigenvector decomposition methods that give the amplitude, azimuth and elevation angle of the three largest components of motion as a function of time. This allows determination of the plane in which acoustic-medium particles move due to dominant acoustic waves. Vector sensor can be used to locate and track an acoustic source. This is illustrated by the test in the semi-anechoic basin and the field tests.

#### 6.1 Basin test

A recording of the accelerometers of the vector sensor during the transmission of a burst-sine signal (5 ms, 3 kHz) in the semi-anechoic tank was used for polarization. All accelerometer channels were fed into the polarization algorithm, where the x-axis was oriented vertically to the water surface. The y-z channels described the motions on the horizontal plane with the z-axis pointing directly to the source. Figure 6.1 shows the calculated azimuth and elevation angles as a function of time. Also the individual acceleration components are shown in the lower figure.

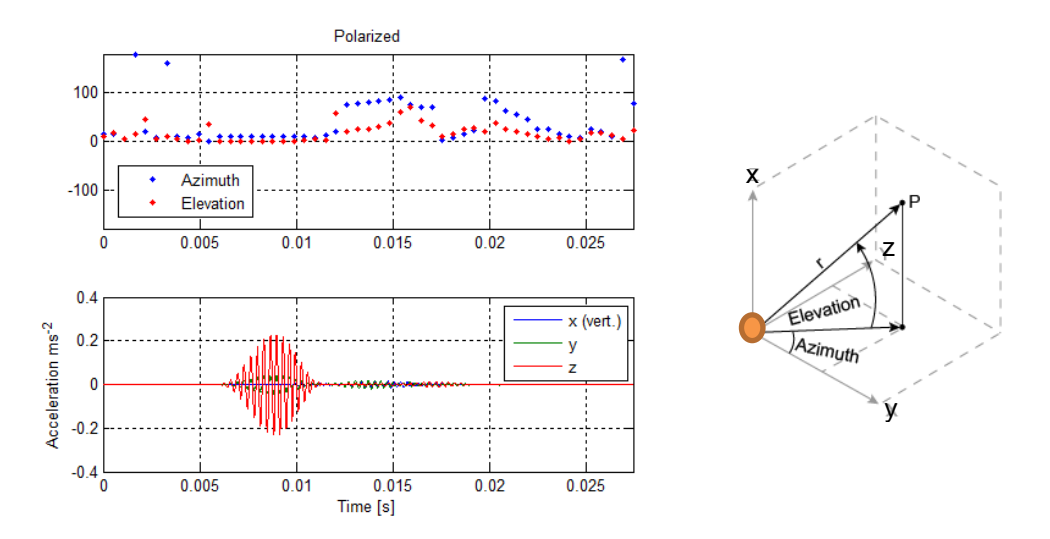


Figure 6.1 Estimated azimuth and elevation angles as a function of time (upper), derived from the three orthogonal acceleration signals (lower).

Before the arrival of the wave front the angles are unstable, indicating that the waves are not coming from a constant direction. During the signal the angles are fixed, pointing out the direction of arrival at about 0 degrees azimuth and elevation angle. When the first reflection comes in the azimuth angle shifts to about 90 degrees, indicating that the reflection is coming from the walls of the basin.

#### 6.2 Field tests

In the field this principle is demonstrated by tracking a moving RHIB at the Haringvliet; see Figure 6.2, and the direction of arrival of the transient noise of a stationary pile driver at the North Sea; see Figure 6.3.

In Figure 6.2 the location of the RHIB can be reasonably tracked with a single vector sensor. The orientation of the coordinate system of the sensor is crucial. Since in this case the orientation had not been measured, the pass-by data in various directions was used to determine its orientation. The offset at start and end of the track is possibly due to an inclination angle of the vector sensor mounting rig on the slope of the sediment.

In Figure 6.3, for the ambient sound part of the recording, prior the pile driver impact, the azimuth angles in the y-z plane (x-direction is vertical) show a large spread, since the sound is coming from many sources from multiple directions. This explains the outliers in Figure 6.3. However when the pile sound wave arrives, the azimuth angle immediately stabilizes at about 40 degrees, which indicates that the sound wave is coming from one specific direction. This can be seen from the first pulse at 2.5 s, prior to the second and third pulses, all related to the piling process. After the first transient at 2.5 s has attenuated, the spread in the angle estimation becomes high. Within this time window the sound is governed by the ambient sources. The angle stabilize again when the second wave front passes the sensor at 3 s. Again the spread becomes higher when the third pulse decays.

The elevation angle is only small, about 4 degrees, but it shows a high variation compared to the azimuth estimation. This could be explained by the fact that the pile driver is a line source.

The exact orientation of the vector sensor in the horizontal plane was unknown. The x-direction was oriented to the water surface, so vertically. The exact orientation of the vector sensor could have been measured with the external heading, roll and pitch sensor, see Chapter 7.

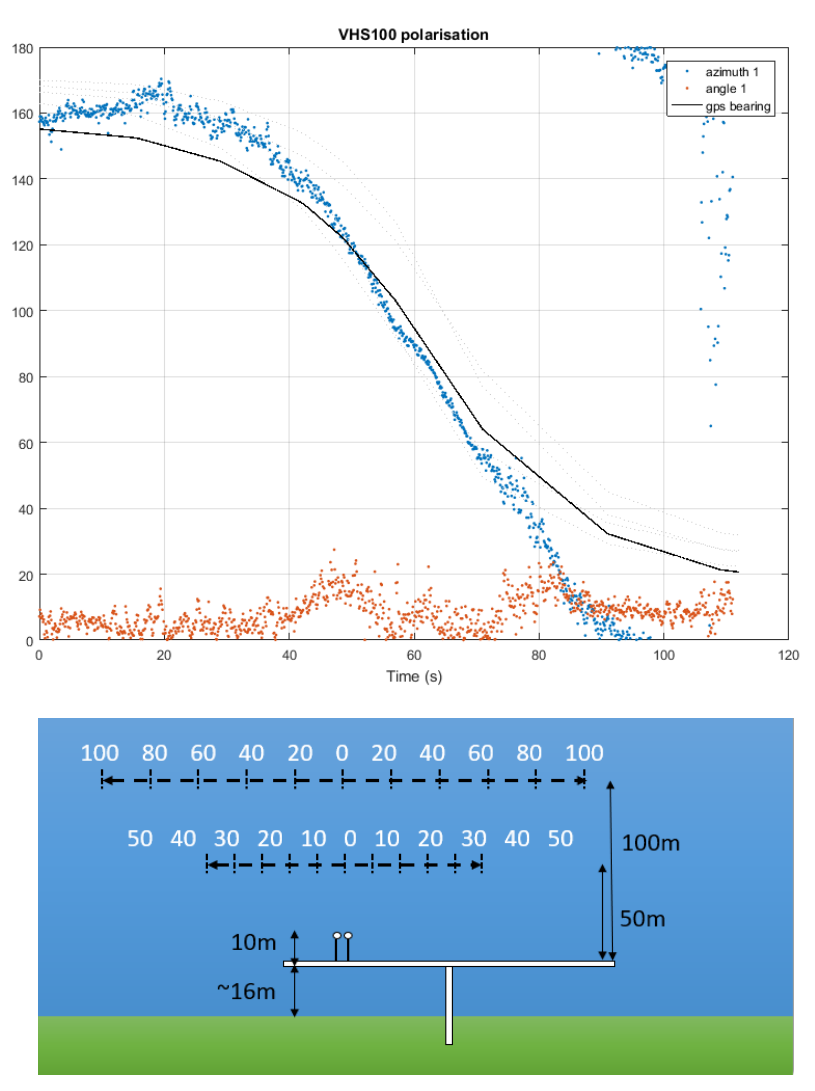


Figure 6.2 Top: The bearing angle as a function of time as obtained from the polarization algorithm is compared to the actual recorded GPS bearing of the RHIB, passing-by at about 100 m distance.

Bottom: the track of the RHIB relative to the pier.

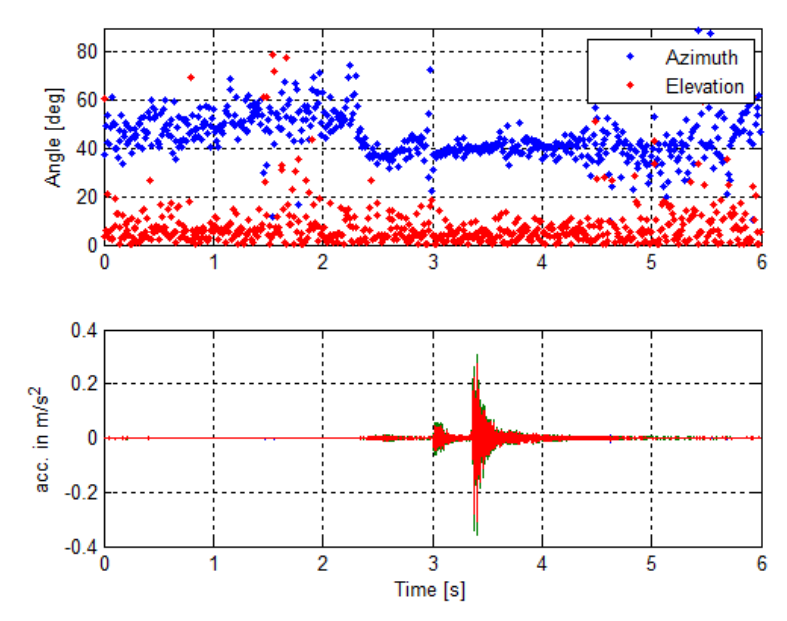


Figure 6.3 Elevation and azimuth angle as a function of time for the pile driver signal, obtained from a 3D particle acceleration measurement.

# 7 Stand-alone vector sensor recording system

The previous chapters describe how the vector sensor can be used successfully using the standard setup, in which the sensor is connected to a data-acquisition system at the surface on land or on board a ship. The measurements are started and stopped using a laptop and the data stored directly. This method requires a sensor position close to the land or a ship which means that the position cannot be freely chosen. Also, it was shown that deployment of a vector sensor from a surface float results in high background sound particle acceleration levels at low frequencies. This is a result of wave induced accelerations which are also picked up by the sensitive sensor.

Therefore in addition to the standard setup a stand-alone setup was also developed and tested. The benefit of a stand-alone system is to be able to monitor particle motion at remote locations over longer periods of time. This means that the location can be chosen more freely, the risk of disturbance due to ship self-noise such as engine noise is reduced and measurements can be performed very close to a source, like a pile driver, where ships are not allowed.

## 7.1 Technical description

For the setup of the stand-alone measurements the 4 channel recording system of RTsys<sup>2</sup> is used (type EA-SDA14). This recording system consists of a separate battery module and a recorder module which are waterproof up to at least 200 m water depth. Because the recorder and the sensors need to be connected underwater also a special watertight connector was developed for the sensor. Also the vector sensor requires a power supply (2\*12 V battery). Therefore a special watertight battery pack was designed that is connected to the new connector of the sensor. All parts of the setup are attached to a stiff cage structure to make the system stable and deployable; see Figure 7.1.

As explained in the previous sections the sensor has three particle motion sensors in different directions. This gives the possibility to define the direction of the sound wave. To be able to use this functionality the orientation of the sensor should always be known. Therefore for the stand-alone system a separate sensor was purchased to log the direction relative to the earth's magnetic field, roll, pitch, water temperature and the water depth.

<sup>&</sup>lt;sup>2</sup> https://rtsys.eu/en/underwater-acoustic-recorders/

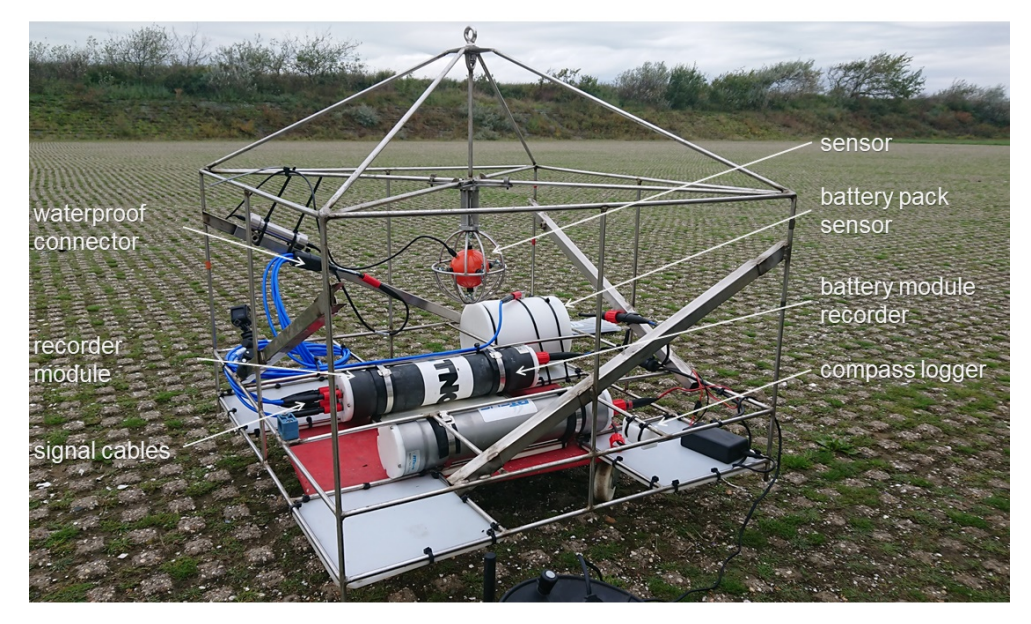


Figure 7.1 Stand-alone vector sensor setup.

## 7.1.1 Compass logger

As an addition to the standard setup a small subsea compass data logger (DST magnetic of STAR ODDI, see Figure 7.2) was added to determine the orientation of the sensor at all times and therefore give the possibility to use the directivity options of the sensor. Besides the orientation relative to the earth magnetic field also the temperature, depth, tilt and pitch are logged. It is of utmost importance to know the exact orientation of the vector sensor's coordinate system on the stand-alone system. The sensor has been tested in the basin and shown to work properly.

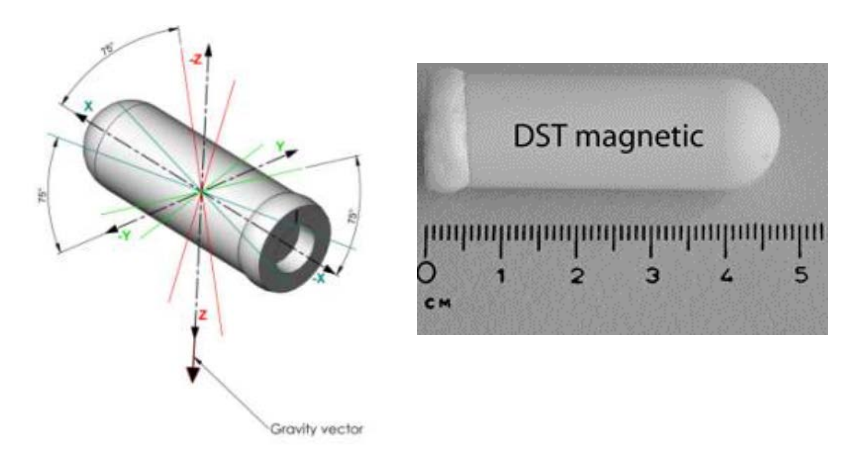


Figure 7.2 Overview of the subsea compass and tilt data logger (DST magnetic of STAR ODDI), dimensions 15 mm by 46 mm.

#### 7.2 Calibrations

Because the RTsys recorder is a different acquisition system than the B&K system used before, another calibration was performed. The same procedures were followed as described in paragraph 4.1.1 Shaker Method and Paragraph 4.1.2.

#### 7.2.1 Shaker Method

The vector sensor was put onto an electro dynamic shaker, without the suspension system. A calibrated reference accelerometer (B&K 4517-002) was mounted to the outer shell of the sphere by bee-wax. The vector sensor was excited by the shaker with a swept-sine from 10 Hz - 10 kHz. From the transfer function from the reference accelerometer to the vector sensor accelerometer voltage in the concerning direction, the sensitivity was derived, see Figure 7.3. The signals were recorded using the RTsys recorder and the results compared to the results of the recordings with B&K Pulse system; see Figure 7.4.

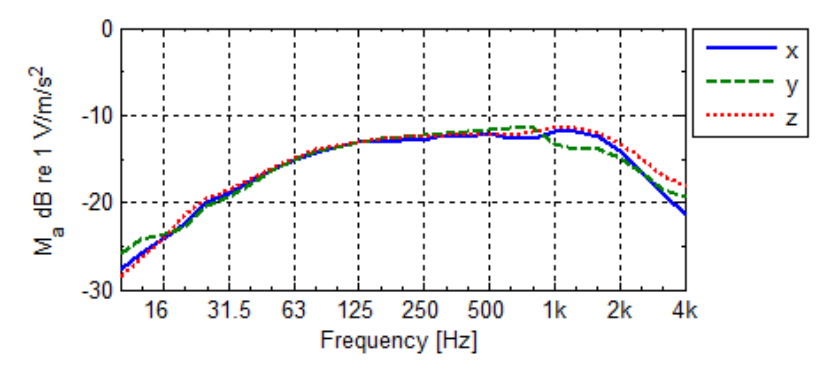


Figure 7.3 Sensitivity of the accelerometers in the vector sensor using the RTsys recorder system.

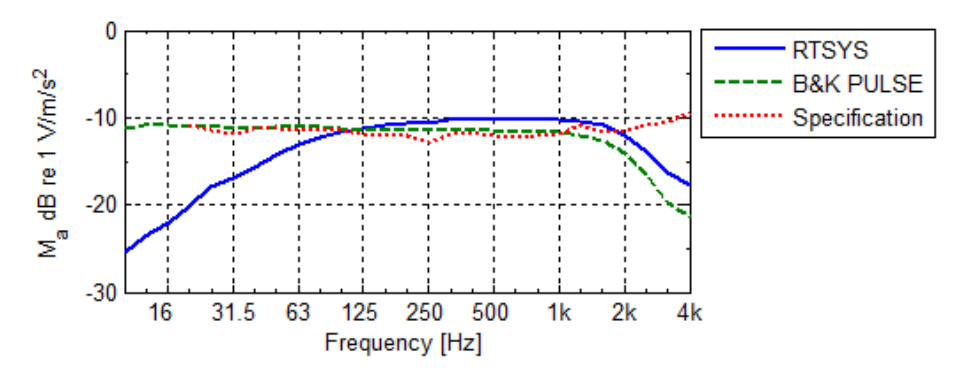


Figure 7.4 Comparison between the results using the B&K recorder system and the RTsys recorder system.

The results show that all accelerometer channels show a comparable sensitivity. The comparison between the B&K recorder system and the RTsys recorder system shows a good agreement above 125 Hz, although the sensitivities obtained from the RTsys recorder are 1-2 dB off specification. For frequencies below 125 Hz the drop-off is caused by the internal high-pass filter in the RTsys recorder (1st order high-pass -3 dB@56 Hz). Measured sound particle acceleration levels need to be corrected for this filter.

#### 7.2.2 Basin

Also the system was calibrated in the basin using the comparison method of Section 3.3. Only the x and y directions in the horizontal plane were tested. Results are shown in Figure 7.4 and Figure 7.5 and are close to specifications.

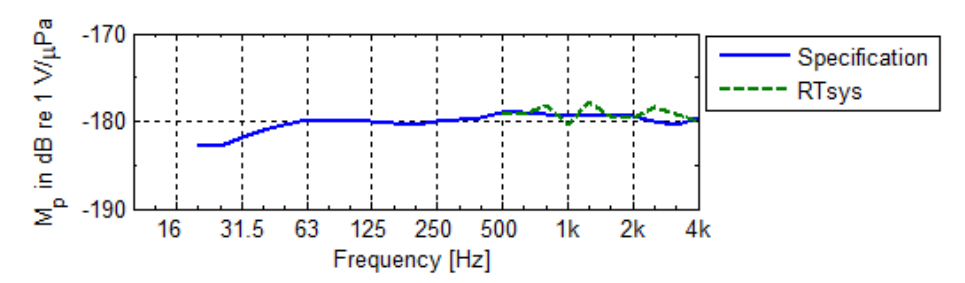


Figure 7.5 Sensitivity of the vector sensor on the RTsys system to sound pressure. The specified sensitivity is -178 dB re 1 V/µPa.

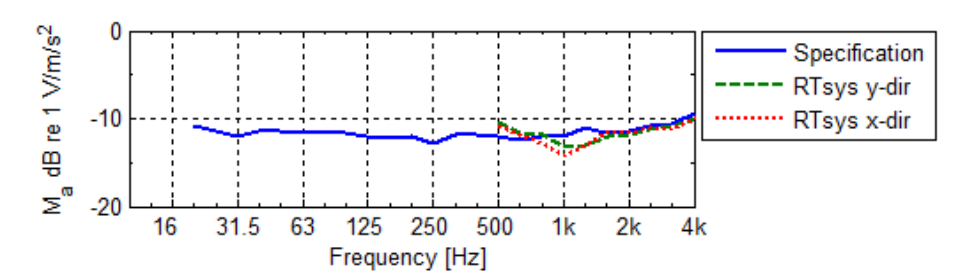


Figure 7.6 Sensitivity of the vector sensor on the RTsys system to sound particle acceleration. The specified sensitivity is -12 dB re 1 V/ms<sup>-2</sup>.

#### 7.2.3 Self-noise measurements

Figure 7.6 shows the background sound pressure and particle acceleration levels of the VHS-100 vector sensor with the RTsys recorder. The tone at 125 Hz is actual sound present inside the basin.

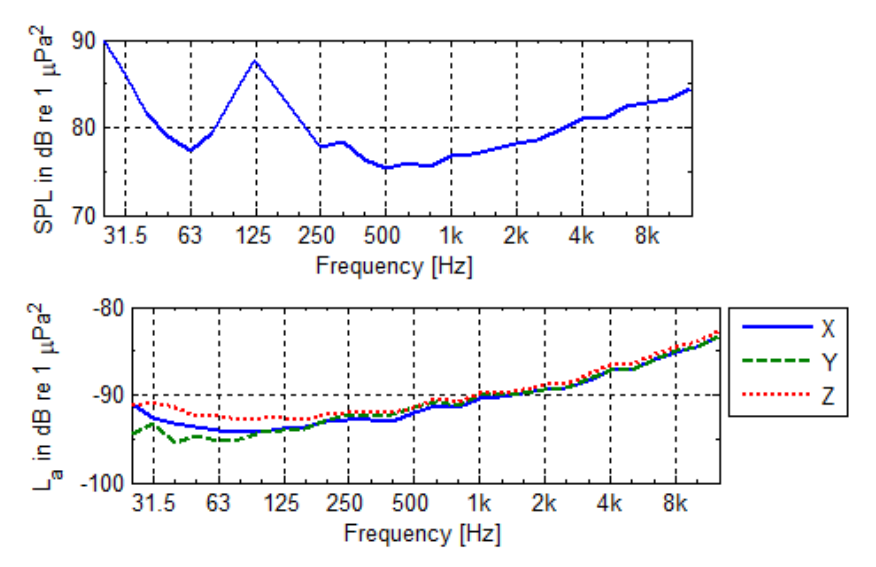


Figure 7.7 Background noise levels for the hydrophone channel (upper) and the accelerometer channels (lower) in third-octave bands.

# 7.3 Field test

In addition to the calibration of the data acquisition systems, the performance of the stand-alone system was assessed by means of an endurance test; see Figure 7.8. An important feature of a stand-alone system is the fact that it can perform long-term measurements. The capacity of the system depends on two factors. The

battery will be empty after some time or the memory of the system will be full. Different endurance tests are created do define performance. Different settings of the system in terms of duty cycle, recording mode and sample frequency were used.

Table 7.1 shows results of the endurance tests for different settings. The recording mode refers to the possibility to save the data on the SD-card (118 GB free for data storage), on the hard disk (214GB free for data storage) or a hybrid mode. The hybrid mode uses the SD-card to store the data during recording and once the recording period has finished, the recorder saves the data to the hard drive. This mode consumes less energy for long term deployment.

The sample frequency refers to the number of data points per second and depends largely on the required bandwidth. The higher the sample frequency the more data has to be saved per second and the sooner the memory of the disks will be full. It is possible to set a duty cycle for the measurements. This means that the recorder will not be measuring all the time, but at defined intervals only. The active time and the passive time can be set separately.

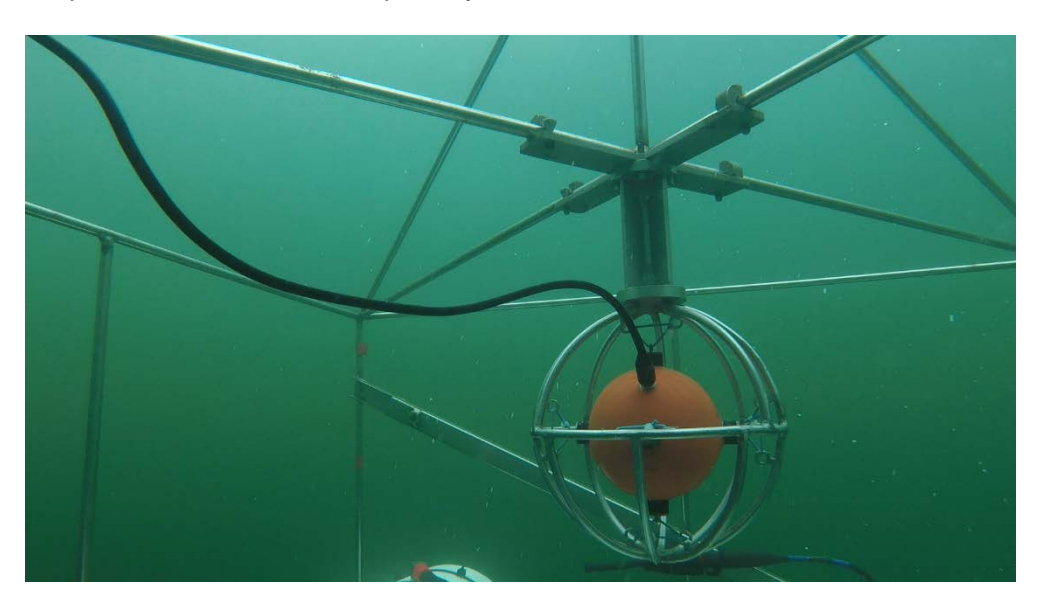


Figure 7.8 Close-up of the submerged vector sensor during stand-alone measurements at Grevelingen.

	Setup	Recording mode	Duty cycle	Sample frequency [Hz]	Constraint	Recording time [h]
1	Dry	Hybrid	100%	39063	Memory	75
2	Dry	Hybrid	50% (5min - 5min)	39063	Battery	290 (145)
3	Dry	Hybrid	50% (1min - 1min)	78125	Battery	188 (94)
4	Wet	SD-Card	100%	39063	Memory	75

In the first measurement the hybrid mode was used in combination with a 100% duty cycle. It has been found that this is not possible because the hybrid mode replaces the data from the SD-card to the HDD after the recording is finished and this only occurs if the SD-card is full. Using a different duty cycle of 50%, with 5 minutes on and 5 minutes off, does work with the hybrid mode and results in a

considerably longer recording time. On the other hand the 50% duty cycle with 1 minute on and 1 minute off does not work in combination with the hybrid mode due to the fact that one minute is not enough time for the recorder to replace the data to the HDD. Therefore the measurement was not started exactly every minute.

The higher the sample frequency is, the more data is collected and the more energy is needed from the battery. Doubling the sample frequency results in an decrease of recording time by 30%.

The measurements with 50% duty cycle show that a measurement time of about 290 hours in possible. This means that there is data for half this period of time. With a 100% duty cycle a measurement of 75 hours is possible. This can be magnified by using a larger SD-card or HDD.

# 8 Conclusions

#### Vector sensor

The measurement of underwater sound for the purpose of environmental impact studies often involves only the measurement of sound pressure by means of a single hydrophone. Measurements of the particle motion induced by sound waves are less often carried out and the equipment necessary to make these measurements is not as widely used. This is justified for research on marine mammals which are sensitive to sound pressure in water like land mammals are for sound pressure in air. However, some species of fish and invertebrates are also sensitive and responsive to particle motion, especially in terms of the acoustic particle acceleration at low frequency. It has become common practice to estimate particle motion from measurements of the sound pressure or its gradient, using rather simple models following the straightforward relationships for a plane-wave propagating under free-field conditions. This conversion is subject to large errors since these conditions hardly ever occur close to reflecting boundaries, like the sea surface or the seabed, in shallow waters. For these conditions, in absence of validated acoustic models, measurement of the particle motion with a dedicated vector sensor is required.

The Acoustics and Sonar department of TNO owns a vector sensor, with a 20 Hz - 4 kHz frequency range , which has been successfully calibrated, so that the sensor is operational. The sensor is an inertial motion sensor, which physically measures the movement of the water in the presence of a sound field by using accelerometers mounted within a rigid freely moving spherical shell. The vector sensor of TNO can be used in bio-acoustic projects in the field of the sensitivity of wildlife to acoustic particle motion generated by anthropogenic sound sources in the sea.

The vector sensor can also be connected to a 4-channel stand-alone recording system, mounted on a cage structure which can be deployed on the seabed. This way of deployment results in much lower background sound particle acceleration levels at low frequencies compared to a system connected to a surface float. This is because the sensitive accelerometers also pick-up all wave induced accelerations. To determine the orientation of the vector sensor's coordinate system, an external compass sensor logger is co-located with the vector sensor. This is of utmost importance for the estimation of the absolute direction of arrival of incoming sound waves.

#### Calibration procedures

At the start of the project no standardized calibration methods for vector sensors existed. Therefore a calibration procedure for vector sensors has been defined and applied on two different vector sensors. The proposed procedure applies two methods for different frequency ranges:

- Shaker method in air (dry calibration) for lower frequencies (20 Hz 1 kHz);
- Comparison method in water (wet calibration) for higher frequencies (500 Hz – 4 kHz).

For vector sensors with a high specific gravity, the results of the dry calibration need to be corrected for the buoyancy effect in order to obtain the correct sensitivity of the

submerged sensor to particle motion. If a vector sensor is close to neutrally buoyance this effect can be neglected.

#### Field test data

Practical data on natural levels and directional components of particle motion in different aquatic environments have been collected to study the conversion of sound pressure measured with a single hydrophone to particle motion assuming plane wave conditions. The cases in shallow waters show that this conversion is subject to large errors for frequencies for a point source below 1 kHz. There are circumstances where the level of particle motion is either larger or smaller for a given sound pressure; for example, close to a source, in waveguides or near boundaries. For these conditions, in the absence of validated acoustic models, measurement of the particle acceleration with a dedicated sensor is required.

For a line source however, like a pile driver, the calculated particle motion levels were only within 2 dB from the measured levels. This shows a good potential for obtaining an estimate of the particle motion from a single hydrophone reading for a line source.

The scaled impedance metric is proposed as a convenient way to quantify the sound pressure – particle motion conversion as a function of range, frequency and depth. It varies significantly with receiver depth, but the variation with receiver distance from the source is much less.

The field tests covered in this report are only a selection of relevant acoustic source type, aquatic environments and distances from the source in terms of governing wavelength. In order to define general recommendations on when to obtain particle motion from single hydrophone measurements in bio-acoustic studies, more relevant cases are to be studied.

# 9 References

- [1] Theobald, P. & Pangerc, T., Review Of Methods For The Calibration Of Vector sensors For The Measurement Of Underwater Acoustic Fields, NPL Report, April 2016.
- [2] Gray, M. D., Acoustic particle motion measurement for bio-acousticians, Proceedings of Meetings on Acoustics, Vol. 27, 010022 (2016).
- [3] Hearing and water column use in North Sea fishes: a review to serve exploration of variation in exposure to vessel sounds among species and species groups, Niels Bouton, Hans Slabbekoorn & Anthony Hawkins IBL-report for TNO for the EU SONIC-project, Leiden University, the Netherlands & University of Highlands & Islands, Scotland, 2015.
- [4] Gray, M.D., Rogers, P.H. & Zeddies, D.G., Acoustic particle motion measurement for bio-acousticians: principles and pitfalls, Fourth International Conference on the Effects of Noise on Aquatic Life, Dublin, Ireland, 2016.
- [5] Isaev, A. E., Matveev, A. N. Nekrich, G. S. & Polikarpov, A. M. (2013) Free Field Calibration of a pressure gradient receiver in a reflecting water tank using a linear frequency modulated signal. Acoustical Physics, 59, 6, pp. 722–729.
- [6] Isaev, A. E., Matveev, A. N. Nekrich, G. S. & Polikarpov, A. M. (2014) Complex calibration of a pressure gradient receiver using the reciprocity method procedure. Acoustical Physics, 60, 1, pp. 45–51.
- [7] Methods for the calibration of vibration and shock transducers Part 21: Vibration calibration by comparison to a reference transducer, ISO\_16063-21\_2003(en).
- [8] Robinson, S. & Hayman, G., Phase calibration of hydrophones by the free-field reciprocity method in the frequency range 10 kHz to 400 kHz, NPL REPORT AC 1, 2007.
- [9] Basten, T.G.H. & de Bree, H.E., Full bandwidth calibration procedure for acoustic probes containing a pressure and particle velocity sensor, J. Acoust. Soc. Am. 127 (1), January 2010.
- [10] Martin, B., Soundscape Characterization and Marine Mammal Presence on the Eastern Grand Banks, NF, P001288-002 Document 01305, JASCO Applied Sciences October 2017.
- [11] Jansen, E., Prior, M. & Brouns, E., On the conversion between sound pressure and particle motion, Proceedings of Meetings on Acoustics, special issue Aquatic Noise conference of the Acoustical Society of America, to be published in 2020.
- [12] ISO 18405:2017 Underwater acoustics Terminology.
- [13] Montalbetti, J. F. & Kanasewich, E. R., "Enhancement of teleseismic body phases with a polarization filter." Geophysical Journal International 21, no. 2 (1970): 119-129.
- [14] Jansen, H.W. & Wilcoxon VS-301 vector sensor, memorandum TNO 2019 M12055, ITAR restricted.

# 10 Signature

The Hague, December 2019

Drs. C.M. Ort Research manager TNO

Acoustics & Sonar

Ir. H.W. Jansen

Author